



Soil and plant phytoliths from the *Acacia-Commiphora* mosaics at Oldupai Gorge (Tanzania)

Julio Mercader^{1,2}, Siobhán Clarke¹, Mariam Bundala^{1,3}, Julien Favreau¹, Jamie Inwood¹, Makarius Itambu^{1,3}, Fergus Larter¹, Patrick Lee^{1,4}, Garnet Lewiski-McQuaid¹, Neduvoto Mollel⁵, Aloyce Mwambwiga^{1,6}, Robert Patalano¹, María Soto¹, Laura Tucker¹ and Dale Walde⁷

¹ Department of Anthropology and Archaeology, University of Calgary, Calgary, Canada

² Department of Archaeology, Max Planck Institute for the Science of Human History, Jena, Germany

³ Department of Archaeology and Heritage Studies, University of Dar es Salaam, Dar es Salaam, Tanzania

⁴ Department of Anthropology, University of Toronto, Toronto, Canada

⁵ Tropical Pesticides Research Institute, National Herbarium of Tanzania, Arusha, Tanzania

⁶ Arusha National Natural History Museum, Arusha, Tanzania

⁷ ASM Research Group, Cochrane, Canada

ABSTRACT

This article studies soil and plant phytoliths from the Eastern Serengeti Plains, specifically the *Acacia-Commiphora* mosaics from Oldupai Gorge, Tanzania, as present-day analogue for the environment that was contemporaneous with the emergence of the genus *Homo*. We investigate whether phytolith assemblages from recent soil surfaces reflect plant community structure and composition with fidelity. The materials included 35 topsoil samples and 29 plant species (20 genera, 15 families). Phytoliths were extracted from both soil and botanical samples. Quantification aimed at discovering relationships amongst the soil and plant phytoliths relative distributions through Chi-square independence tests, establishing the statistical significance of the relationship between categorical variables within the two populations. Soil assemblages form a spectrum, or cohort of co-occurring phytolith classes, that will allow identifying environments similar to those in the *Acacia-Commiphora* ecozone in the fossil record.

Submitted 28 August 2019
Accepted 14 November 2019
Published 11 December 2019

Corresponding author
Julio Mercader,
mercader@shh.mpg.de,
julio.mercader@gmail.com

Academic editor
Ian Moffat

Additional Information and
Declarations can be found on
page 28

DOI 10.7717/peerj.8211

© Copyright
2019 Mercader et al.

Distributed under
Creative Commons CC-BY 4.0

OPEN ACCESS

Subjects Anthropology, Ecology, Evolutionary Studies, Soil Science

Keywords African palaeoenvironments, Soil and plant phytoliths, *Acacia-Commiphora* woodland and grassland mosaics, Reference collections, East Africa, Analog for early human evolution

INTRODUCTION

Multiple proxies indicate that during the last two million years the East African climate changed, triggering a shift in its plant landscape from forested ecosystems to open woodland/grassland mosaics. These proxies include paleosol carbonates (*Cerling, Bowman & O'Neil, 1988; Levin et al., 2004; Quinn et al., 2007; Levin et al., 2011*), vertebrates (*Bibi & Kiessling, 2015; Bibi et al., 2018; Prassack et al., 2018*), palaeobotanical remains (*Bonnefille, 1984; Bonnefille, 1995*), and stable isotopes (*Magill, Ashley & Freeman, 2013a; Magill, Ashley & Freeman, 2013b; Uno, Polissar & Jackson, 2016; Lupien et al., 2018*). This environmental transformation led to the widespread occurrence of a plant landscape characterized

by *Acacia-Commiphora* woodland (White, 1983), and corresponds with key changes in hominin evolution and ecology (e.g., Ravelo et al., 2004; Lepre et al., 2011; Beyene et al., 2013).

Over the last few decades, different investigations have attempted to identify modern ecosystems as referential correlates for Pleistocene East African vegetation communities within the Somalia-Masai floristic region; a center of endemism that extends over 2 million km² in parts of Ethiopia, Sudan, Uganda, Kenya, and Tanzania. For example, lakes such as Manyara and Makat are often considered correlates for paleo-Lake Oldupai as they have vegetation types not in equilibrium with the regional climate (Barboni, 2014; Copeland, 2007). Peters & Blumenschine (1995) developed a paleolandscape model that predicted possible hominin land use patterns based on reconnaissance surveys in eastern and southern Africa. Copeland (2007) examined habitats in northern Lake Manyara, Ngorongoro, and the Serengeti Plain as baseline to understand the paleolandscape inhabited by early *Homo* in terms of climate, land forms, and soil types.

At present, there is no extensive, ecosystem-wide phytolith analog for the *Acacia-Commiphora* landscape that was the backdrop for human evolution in some regions of East Africa over the last two million years (Bobe & Behrensmeyer, 2004; Plummer et al., 2009; Cerling et al., 2011; Blumenthal et al., 2017). Researchers have focused instead on a variety of microhabitats such as groundwater-fed woodlands (e.g., Ashley et al., 2010; Barboni et al., 2010), mosaic fluvial systems (e.g., Arráiz et al., 2017), and lake-shore palm groves (Albert, Bamford & Cabanes, 2009; Albert, Bamford & Esteban, 2015).

In Quaternary palaeoecology, phytolith analysis has successfully addressed evolutionary and environmental questions (see review in Strömberg et al., 2018). Phytoliths are microscopic silicifications mirroring the morphometric characteristics of the plant organs where they precipitate, inside and between plant cells of varied groups (Rovner, 1971; Piperno, 1988; Hodson et al., 2005; Hodson, 2016; Strömberg, Di Stilio & Song, 2016). Phytogenic silica is released into soils after litter decomposes and discharges both amorphous silica and phytoliths. This process creates a synchronous phytolith record of the plant communities that grew in the soil (Piperno & Becker, 1996; Kerns, Moore & Hart, 2001; Clarke, 2003; Piperno, 2006; Thorn, 2006; Honaine, Zucol & Osterrieth, 2009; Morris, Ryel & West, 2010; Mercader et al., 2011; Novello et al., 2012; Novello et al., 2018; Blinnikov, Bagent & Reyerson, 2013; An, Lu & Chu, 2015; Watling et al., 2016; Esteban et al., 2017; Fick & Evett, 2018).

We explore the soil phytolith assemblages from *Acacia-Commiphora* woodlands to identify similar environmental contexts in the fossil record, undertaking a concurrent study of phytoliths from local plants to aid in taxonomic classification (Wallis, 2003; Carnelli, Theurillat & Madella, 2004; Gallego & Distel, 2004; Bremond et al., 2005; Tsartsidou et al., 2007; Barboni & Bremond, 2009; Mercader et al., 2009; Mercader et al., 2010; Gao et al., 2018a; Gao et al., 2018b). The comparison of soil and plant phytoliths can assist in tracking the boundary between woodlands and grasslands (Kerns, Moore & Hart, 2001; Morris, Ryel & West, 2010; Mercader et al., 2011). Elsewhere, this comparison has been helpful to assess phenomena such as time averaging (Alexandre et al., 1997; Blecker et al., 2006; Mercader et al., 2011; Hyland, Smith & Sheldon, 2013), catchment (Fredlund & Tieszen, 1994; Blinnikov,

2005), and ecological succession (Leakey, 1979; Niboye, 2010) that are hereby studied at the regional and local level.

STUDY AREA

Oldupai Gorge falls within the Northern Tanzania Divergence Zone along the East African Rift System (Dawson, 1992; Foster et al., 1997) (Fig. 1A). It represents the boundary between central Tanzania's Archaean craton and the north-south trending Mozambique belt, a product of the neo-Proterozoic Pan-African orogeny (Holmes, 1951; Cahen et al., 1984). Oldupai Gorge sits on the western flank of the Gregory Rift in the Ngorongoro Conservation Area (2°59'46.87"S, 35°21'7.50"E) between the volcanic highlands to the south and east, the metamorphic complexes to the north, and the Serengeti Plains to the west. Paleolake Oldupai was part of an endorheic basin formed >2 Ma as a result of tectonic subsidence and concomitant uplift in the Ngorongoro Volcanic Highlands (Hay, 1976), where numerous volcanoes existed (Mollet & Swisher III, 2012). Oldupai Gorge boasts well-dated archaeological and fossil records (Leakey et al., 1972; Hay, 1976; Deino, 2012). Its sedimentary beds span the Pleistocene (Beds I–IV, Masek, Ndutu, and Naisiusiu) and situate two million years of evolutionary history, from the Oldowan to the Later Stone Age (Leakey, 1971; Leakey & Roe, 1994).

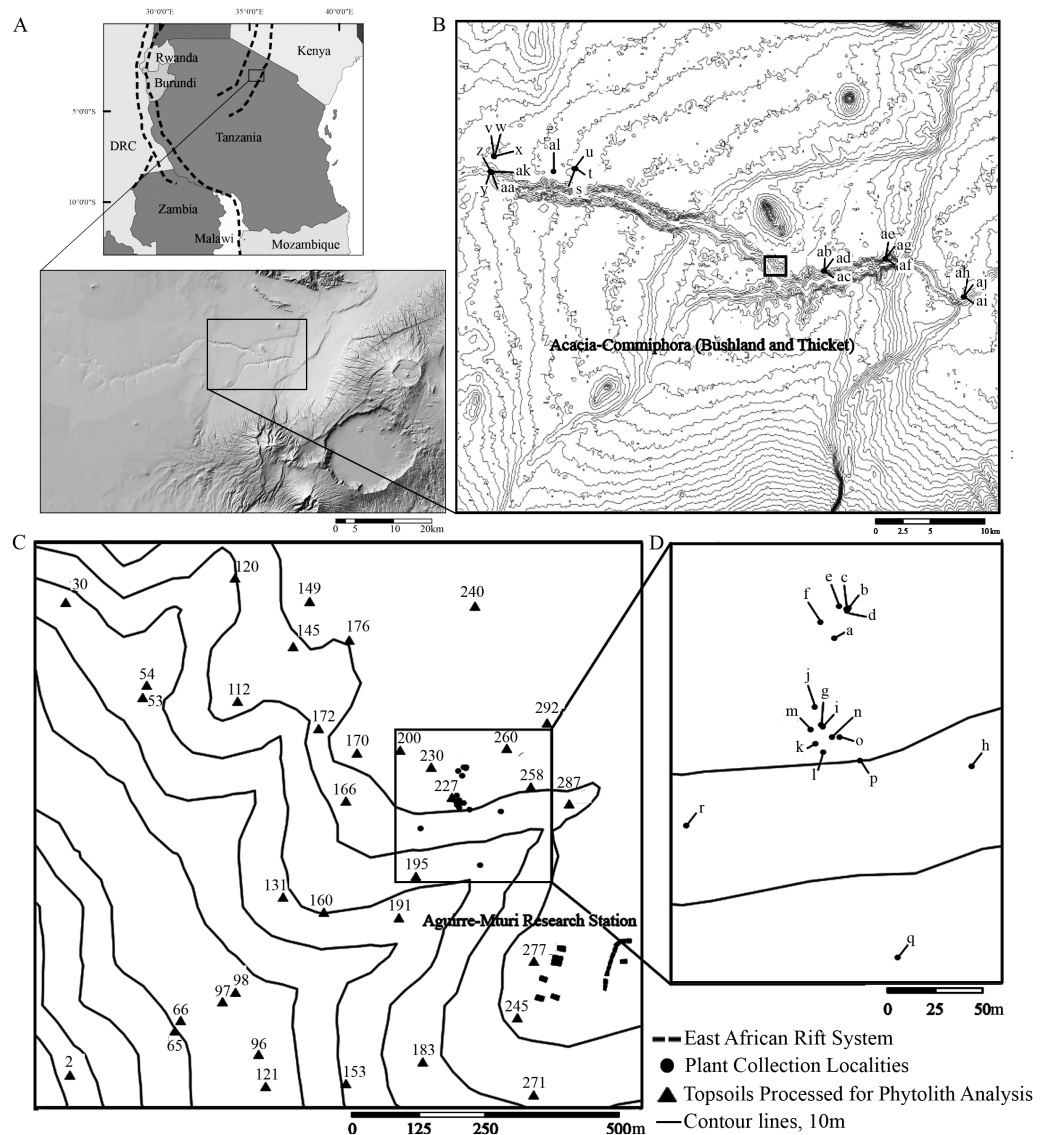
The Eastern Serengeti Plains (Fig. 1) offer a varied topography between 1,350 m–1,550 m above sea level with a central plateau around Oldupai Gorge and highlands toward Endulen, enduring wide temperature oscillations and high winds (Anderson & Talbot, 1965; EAMD East African Meteorological Department, 1967; Norton-Griffiths, Herlocker & Pennycuik, 1975; White, 1983). Annual rainfall ranges from 380 mm to 803 mm per year, but at the Gorge it fluctuates from 331 mm–531 mm (Herlocker & Dirchl, 1972). The dry months in Oldupai Gorge extend from June to October, with the wettest phase lasting from December to April. Rainfall patterns and localized soil conditions influence the vegetation communities observed in the Serengeti (Anderson & Talbot, 1965). The dominant soils are calcimorphic, yellowish brown, with low humic values (<1% organic carbon) and a hard pan (Anderson & Talbot, 1965).

MATERIALS AND METHODS

The Tanzania Commission for Science and Technology (permit 2018-112-NA-2018-36), and the Tanzanian Ministry of Natural Resources and Tourism, through its Antiquities Division (permit 14/2017/2018) approved this work. Authorities at the Ngorongoro Conservation Area allowed us to enter the protected area (BE.504/620/01/53). The export license for the materials presented in this study were obtained from the Antiquities Division (EA.150/297/01: 5/2018/2019) and the Tanzanian Executive Secretary from the Mining Commission (00001258).

Vegetation survey

The greater Serengeti area falls within the Somalia-Masai floristic region in which *Acacia-Commiphora* deciduous bushland is the climax vegetation (Kindt et al., 2011).



Full-size [DOI: 10.7717/peerj.8211/fig-1](https://doi.org/10.7717/peerj.8211/fig-1)

This ecoregion is transitional to miombo woodlands to the south (Frost, 1996) and the Zanzibar Inhambane coastal forest mosaic to the east (Lovett & Wasser, 1993). The published plant inventory for Oldupai Gorge totals 32 genera (Herlocker & Dirchl, 1972). We studied 29 species representing 20 of these genera and 15 families. Characteristic Somalia-Masai taxa analysed here comprise the dominant members of the canopy (*Acacia mellifera*, *A. nilotica*), emergents (*Boscia angustifolia*), bushes (*Barleria eranthemoides*, *Maerua triphylla*), the herbaceous layer (*Hypoestes forskoolii*, *Ocimum* spp.), succulents (*Sansevieria robusta*, *Aloe secundiflora*), and the grasses (*Sporobolus consimilis*, *Cynodon dactylon* -Chloridoideae, *Aristida adoensis* - Aristidoideae).

Vegetation in the greater Oldupai region has been monitored for decades (Niboye, 2010). The average perennial cover today is 22% (Niboye, 2010), which is comparable to that observed several decades ago (Anderson & Talbot, 1965), with bare terrain exposing >45% of the area. Herlocker & Dirchl (1972) noticed an increased plant variety in the eastern sector of the gorge, introduced by the topographic changes from the canyon walls, and thus a higher diversity of bushes and grasses. They also noticed commonalities with the communities from the western gorge.

Ecologically, the plant community that typifies the natural vegetation at Oldupai Gorge is short *Acacia* and *Commiphora* woodland. Several tree species from these two genera co-dominate along with bushes such as *Barleria eranthemoides*. Succulents abound in ravines and depressions where several species of *Sansevieria*, *Euphorbia*, and *Sarcostemma* are common. Herbaceous plants are variably scattered across the landscape but, overall, they are low in numbers. Importantly, this domain is characterized by a paucity of grass taxa, which are typically inconspicuous and occasional (Kindt et al., 2011).

At the regional level (Fig. 1B) the vegetation was surveyed using qualitative criteria, aimed at investigating the range of species present in the greater Oldupai region, learning about their phytolith production and morphotype characteristics, and comparing the botanical dataset with the soil group. We did not attempt to collect plant specimens in numbers proportionate to frequency in each of their respective ecological communities, nor to other physiognomic variables or phylogenetic affiliation. Instead, we collected representative plants from the western and eastern gorge at the end of the wet season into the dry season in 38 sampling locations to target 29 species along an E-W transect (25 km long) from Granite Falls to Olbabal. Field samples were identified in the National Herbarium of Tanzania at the Tropical Pesticides Research Institute. When species level identification was uncertain and could belong to several species within the genus, we listed it as spp. Grouping and nomenclature come from the index of accepted names for the flowering plants of Sub-Saharan Africa (Klopper et al., 2006).

At the local level, the vegetation was surveyed using quantitative criteria. First, an aerial image covering 1 km² (Fig. 1C) taken at the end of the wet season in the eastern half of Oldupai Gorge, was georeferenced via ArcGIS - ArcMAP 10.5.1. A grid consisting of 100 cells, each 100 m², was superimposed. The cover-abundance value was digitized in each cell as a polygonal shape file, and classified it in four classes or ranks:

- 1) Rank zero, or 'No-cover': when plant cover constituted <10% within the spatial polygon (45.64% of the total area).

- 1) Rank one, or 'Sparse': when plant growth was 10%–20% (20.32% of the total).
- 2) Rank two, or 'Open': when plant growth was 20%–60% (26.41% of the total).
- 3) Rank three, or 'Closed': when plant growth was >60% (7.63% of the total).

This rank system was subjected to groundtruthing in 300 spots ([Mercader et al., 2017: Fig. 2](#)), and then we proceeded to conduct a qualitative vegetation survey of the entire 1 km² plot ([Fig. 1C](#)). After this, we zoomed into a 62,500 m² quadrat ([Fig. 1D](#)) to conduct a full inventory, plotting, and collection of all plants present within this smaller plot. According to plant cover rank ([Fig. 2](#)), thirteen samples (37.14%) were recovered from rank zero; eight (22.86%) from rank one; eight (22.86%) from rank two; and six (17.14%) from rank three. Samples were each assigned to one of two topographical categories: promontory or ravine. Ravines are at a mean elevation of 1,422.66 m with a range between 1,412 m and 1,441 m (29 m). Promontories are at a mean elevation of 1,452.41 m with a range between 1,416 m and 1,469 m (53 m). Most samples ($n = 29$, 82.86%) were recovered from promontory locations ([Fig. S1](#)).

Particle size analysis

We carried out particle size analysis of selected soil samples ($n = 10$) via laser diffraction (Malvern Mastersizer 2000: [Sperazza, Moore & Hendrix, 2004](#)). A soil sample (1.0 g) was deflocculated with 0.1% sodium hexametaphosphate. Ultrasonics dislodged clays for 5 min. Sample was left on orbital shaker overnight at 200 rpm. We cleansed the sample of carbonates, phosphate, and organics via hydrochloric acid (HCl 37%), nitric acid (HNO₃ 60%) and hydrogen peroxide (H₂O₂ 30%) successively, rinsing the sample three times via centrifuging in between each treatment (3,000 rpm, 5 min). When measuring particle size in the Malvern 2000, we used obscuration rates above 15% but below 30%. The measurement of pH in all soils was through a ThermoFisher Orion 320 PerpHecT LogR meter, calibrated daily. The Ag/AgCl electrode was rinsed after calibration and in between samples. Sediment color was estimated dry under constant light conditions by two observers relative to the Munsell color system. Water loss on drying is the balance between soil field moisture in three grams of soil and the mass of the sample after drying at 110 °C for 24 h.

Soil phytoliths

Sampling was never conducted on archaeological sediments, nor within any of the well-known and mapped lacustrine and fluvial outcrops that constitute the ancient beds ([Leakey et al., 1972](#); [Hay, 1976](#)); our work was restricted to purely surficial sandy loam ([Anderson & Talbot, 1965](#)). Prior to collecting soil samples, and to better understand local soils and visualize their horizons, several trenches were dug reaching the C-horizon: a characteristic underlying hard pan described by earlier soil analysts ([Anderson & Talbot, 1965](#); [Jager, 1982](#)). In section, we observed a thin A-horizon, restricted to the rhizosphere and litter zone, while a B-horizon seems absent. We scraped 25 cm² off the surface (5 ml) to a maximum depth of one cm within the A-horizon ([Fishkis, Ingwersen & Streck, 2009](#); [Mercader et al., 2010](#)), excluding litter and not mixing or generating composite samples. Thirty-five loci were selected for stratified sampling, so that a comparable number of samples were collected from each plant cover type. The median distance

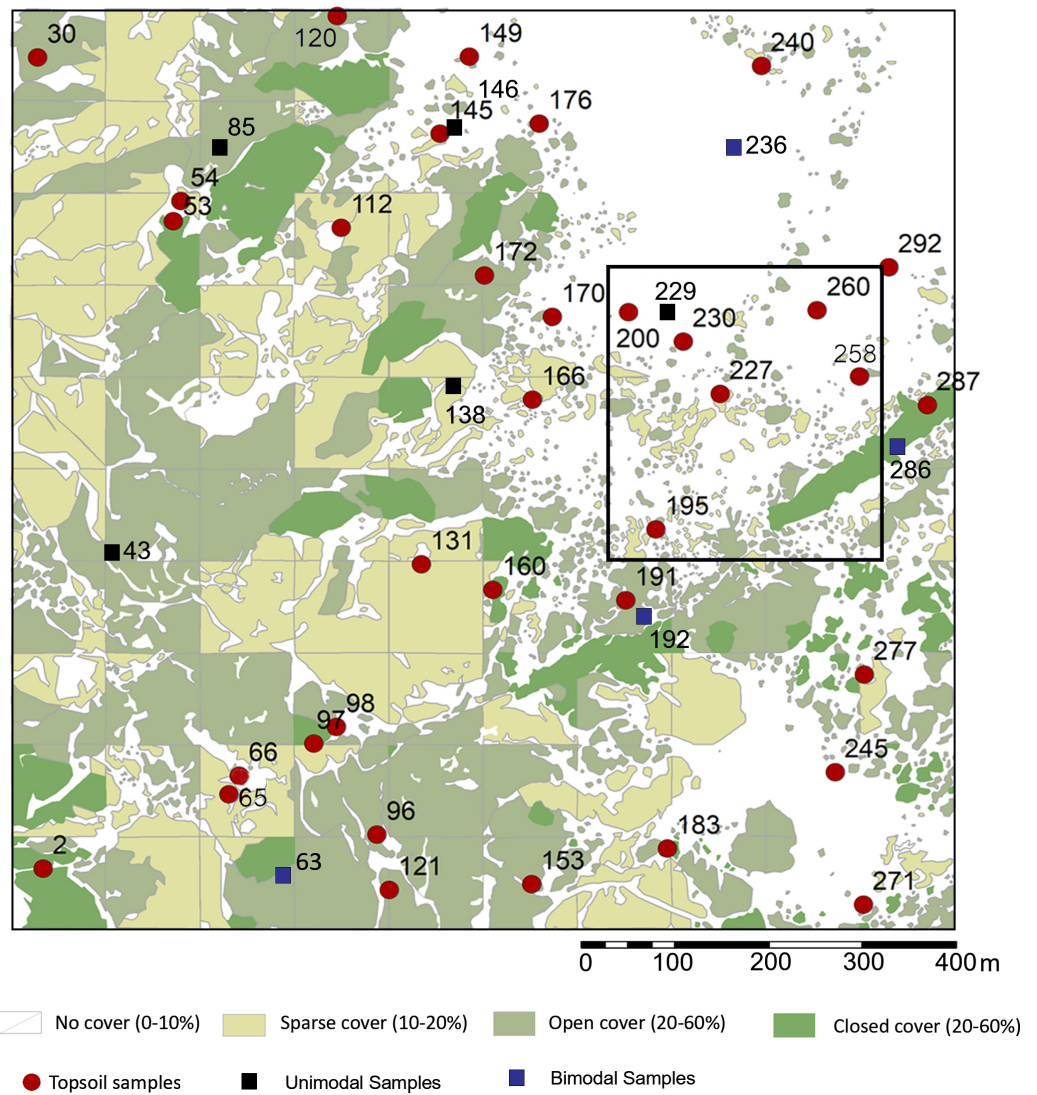


Figure 2 Sampling localities for soils and particle size analysis in relation to plant cover rank, with catchment transect in outline. See Table 1 for analytical description of soils. Digitized source: 2017 ESRI ArcGIS.

Full-size  DOI: [10.7717/peerj.8211/fig-2](https://doi.org/10.7717/peerj.8211/fig-2)

between all soil assemblages is 516 m (measured distances, $n = 522$) over a range of 13 m–1,252 m. Geographical coordinates were documented as point features. The full dataset of soil samples including provenance, elevation, coordinates, processing weights, and individual counts are available at the Federated Research Data Repository (DOI <https://dx.doi.org/10.20383/101.0122>).

Detailed phytolith extraction protocols are available with the Federated Research Data Repository (DOI <https://dx.doi.org/10.20383/101.0123>), which are modified from (Albert *et al.*, 1999). In brief, extraction from sediment used a 3.0 g aliquot that received 10 ml of 0.1% sodium hexametaphosphate for clay dispersion, followed by sonication (15 min) and overnight orbital shaking plus decantation of clays. Samples were rinsed and dried over

two days (>70 °C). Soil samples received 10 ml equal parts 3N hydrochloric and nitric acids; then, rinsed and centrifuged at 3,000 rpm. Drying followed for two days (70 °C). Samples were weighed and transferred to Petri dishes on a hot plate (70 °C) whereby 10 ml of hydrogen peroxide (30%) was added to remove organics. Rinsing, drying, and weighing followed. Phytolith separation was done by transferring this fraction to 15 ml centrifuge tubes, to which 5 ml sodium polytungstate (~2.4 s.g.) was added. Samples were vortexed for five minutes at 3,000 rpm. The supernatant was removed. A gradual decrease in specific gravity over the course of three subsets (subfractions 1, 2, 3) concentrated phytoliths in the third extract. Samples were rinsed with de-ionized water before centrifuging twice more, followed by two cycles of high centrifugation (4,500 rpm). Samples dried at 70 °C another time and a final weight obtained. The aliquot extracted for phytolith analysis weighed approximately 0.001 g. It was mounted with Entellan New and inspected while fresh; allowing particles to be rotated in three dimensions under the microscope. Phytoliths from soil samples were counted on one slide over 600 mm² to the total amount, reaching average counts of 250. Diatoms were tallied concurrently. Carbonate content was calculated as the loss on acid treatment relative to the original mass. Extraction weights are the balance between the original mass and that of the extract after defloculation, carbonate removal, destruction of phosphate, elimination of organics, rinsing, and drying.

Plant phytoliths

Extraction followed *Albert & Weiner (2001)*, with modifications. Botanical specimens were sorted into anatomical parts, and each was individually weighed and measured. Full datasets with species, plant part studied, provenance, elevation, coordinates, processing weights, and individual counts are available at the Federated Research Data Repository (DOI <https://dx.doi.org/10.20383/101.0122>). All samples were cleansed by ultrasonication, then rinsed and dried overnight >80 °C. Dry weight was obtained, and samples placed in a muffle furnace (24 h, 400 °C). The resulting ashes were weighed and transferred to Petri dishes to which 10 ml of 3N hydrochloric and nitric acids were added to a hot plate at 70 °C for 30 min. Samples were transferred to 15 ml tubes and rinsed of remaining acids in three wash and centrifugation cycles at 3,000 rpm, with excess water being boiled off. Hydrogen peroxide (10 ml, 30%) was added to the Petri dishes heated on hot plates (70 °C), transferred to 15 ml centrifuge tubes, rinsed, and centrifuged (3,000 rpm) for three cycles. Samples were dried >70 °C overnight, and then weighed. An aliquot of approximately 0.001 g was analysed after mounting the sample for microscopy with Entellan New. Inspection captured three-dimensional characteristics during rotation conducted within 48 h of mounting and before the resin dried. Frequent polarization of the field of view under the microscope ensured that no anisotropic particles and crystals were confused for phytoliths. Neither fresh nor weather volcanic glass could be observed. We counted one full slide and only discrete phytoliths (average = 106 phytoliths), while articulated shapes were counted as one. As for very rich extracts, we tallied a minimum of 200 phytoliths and/or short cells for the grasses.

Phytolith classification

There are two approaches to environmental reconstruction in phytolith research: the indices (*Barboni, Bremond & Bonnefille, 2007; Bremond et al., 2008*) and the general approach (*Strömberg, 2004*). Different researchers adopt one approach or another depending on their work's practice and scope. We followed the general approach here to detect plant variations at the spatial level. Quantitative analysis involved exploration aimed at discovering relationships amongst the soil and plant phytoliths, which, when combined and filtered, isolated groups, classes, and morphotypes unique to each set and those in common. Further investigation involved comparison of phytoliths from soils and plants to explore their relative distributions through Chi-square independence tests, establishing the statistical significance of the relationship between categorical variables within the two populations using a 95% confidence value ($p = 0.05$).

Two system, polarizing microscopes (Olympus BX51, Motic BA410E) allowed us to confirm the opal silica's isotropy and tally phytoliths at 400x, following the International Code for Phytolith Nomenclature 1.0 to name and describe specimens (*Madella, Alexandre & Ball, 2005*), with exceptions duly noted. Geographically pertinent reference collections and published soil phytolith assemblages were consulted (*Albert, Bamford & Cabanes, 2006; Albert, Bamford & Esteban, 2015; Bamford, Albert & Cabanes, 2006; Fahmy, 2008; Mercader et al., 2009; Mercader et al., 2010; Mercader et al., 2011; Barboni & Bremond, 2009; Eichhorn, Neumann & Garnier, 2010; Novello et al., 2012; Collura & Neumann, 2017; Neumann et al., 2017*). Full datasets with individual counts for each morphotype are available at the Federated Research Data Repository (DOI <https://dx.doi.org/10.20383/101.0122>). We classified discrete phytolith shapes in four large groups (woody dicot, grass short cells, generic Poaceae, and rare) and 17 classes that encompass 76 types. The woody dicot group totalled the blocky class (*Mercader et al., 2009; Novello et al., 2012; Collura & Neumann, 2017*), cylindrical types from bark (*Mercader et al., 2009*), varied globular phytoliths (*Runge, 1999; Mercader et al., 2009*), tabular types from woody dicots (*Mercader et al., 2009; Collura & Neumann, 2017*), clavates (*Mercader et al., 2009*), and sclereid phytoliths (*Collura & Neumann, 2017*). Phytoliths from Poaceae short cells were subdivided in three classes: lobate (*Fahmy, 2008; Neumann et al., 2017*), rondels (*Mercader et al., 2010; Novello et al., 2012; Neumann et al., 2017*) and chloridoid saddles (*Twiss, Suess & Smith, 1969; Mercader et al., 2010*). Two additional groups comprised generic grass phytoliths and rare morphotypes.

It should be noted that the tabular class, with 12 shape variants, contains a confuser morphotype called here tabular sensu stricto, and defined as a narrow, thin parallelepiped shape with straight edges that may occur in both monocots and dicots. This confuser morphotype differs from the tabular psilate observed in woody dicots (this study) in that the latter is a wide and thick tabular shape with a very slight sinuosity to the outline.

Table 1 Particle size analysis of selected topsoils, textural classification, phytolith-bearing fraction, modality, pH, color, and water content.

Sample	Mean particle size, μm	Particle class	Silt & Very Fine Sand, %	Modality	Sediment pH	Sediment colour	Sediment H ₂ O content, %
43	294.2	Medium sand	39.62	Unimodal	8.7	Dark yellowish brown	3.9
63	513.8	Coarse sand	22.73	Bimodal	8.3	Moderate yellowish brown	5.4
85	216.9	Fine sand	49.49	Unimodal	8.8	Dark yellowish brown	6.5
138	94.7	Very fine sand	72.86	Unimodal	8.7	Dark yellowish brown	3.6
146	335.8	Medium sand	38.33	Unimodal	9.1	Pale yellowish brown	3.7
192	469.6	Medium sand	37.59	Bimodal	8.6	Moderate yellowish brown	2.7
229	322.1	Medium sand	26.31	Unimodal	8.7	Dark yellowish brown	2.8
236	670.3	Coarse sand	17.75	Bimodal	8.4	Dark yellowish brown	3.7
279	736.8	Coarse sand	6.54	Unimodal	9.2	Dark yellowish brown	2.9
286	300.1	Medium sand	35.52	Bimodal	8.6	Dark yellowish brown	4.0
Mean	344.3	Medium sand	29.55	Unimodal	8.7	Yellowish brown	3.8

RESULTS

Soil phytoliths

Soil characteristics and phytolith abundance

Local topsoils (Table 1) have a mean particle size of 344 μm , with pH of 8.7 and 5% water content. Unimodal particle size distribution is apparent in the poorly sorted soil matrices of most samples, while the coarse sand component in samples from the eastern half of our plot generates a bimodal population in which the poorly sorted fines represent the soil, and the well-sorted, coarse sands originate from easterly aeolian import (Fig. 3). Silt and very fine sands average 34% per sample, while carbonates are 69% by mass. The extracted phytolith-bearing fraction, which includes both biogenic and geogenic silica, is 54.53% ($M = 53.85\%$; range = 45.54%, 25.23%–70.77%). Dissolution and mechanical breakage were rarely observed, and caution must be used not to confuse the effect of dissolution causing holes randomly through a phytolith versus the cavate textures that heavily decorate some blocky and tabular morphotypes (Figs. 4Q, 4W) from woodland taxa (cf. Mercader *et al.*, 2009: Fig. 6g,k,l,m).

No soil sample was void of phytoliths. In total, 10,745 phytoliths were tallied ($\bar{X} = 307$, $M = 285$ per sample; range = 839, 16–855) containing 64 morphotypes that can be grouped into 15 major classes (Fig. 4, Table 2). Of these, six are prominent classes (Figs. 5, 6) and account for 83.78% of all soil phytoliths: tabular: 41.74%, blocky: 13.11%, globular: 8.52%, rondel: 6.98%, cylindrical: 6.96%, and lobate: 6.47%. Within the tabular class, the three most prominent contributors represent 82.16% of the subtotal: scrobiculate: 45.40%; sinuate: 20.47%; and thick lacunate: 16.30%. Two types of blocky phytoliths represent 91.12% of the class; blocky: 62.38% and ridged: 28.74%. One single type of globular phytolith represents 85% of all globular types: a globular to hemispherical, facetate body with a centric cavity; possibly from mesophyll cells found in the leaves from several taxa in the Lauraceae (Figs. 4A and 4D; Thorn, 2001; Murungi, 2017). In contrast, the classic indicator of arboreal cover in the African tropics, the globular granulate, amounts to only 9% of the globular class. Two globular morphotypes were recovered from soils only: globulose bisected and

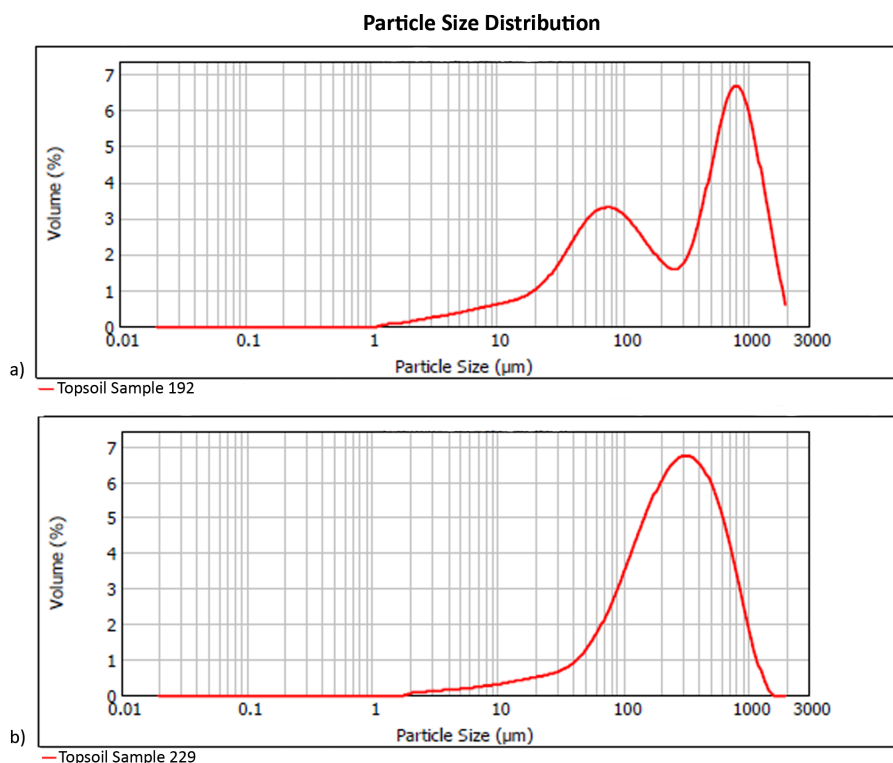


Figure 3 Particle size distribution examples (A) bimodal (Sample 192), and (B) unimodal (Sample 229). Refer to Table 1 for complete sample characterization, and Fig. S1 for sampling location. Digitized 2017 ESRI ArcGIS.

Full-size DOI: [10.7717/peerj.8211/fig-3](https://doi.org/10.7717/peerj.8211/fig-3)

segmented. Within the cylindrical class, two phytoliths reach 91.44%: scrobiculate, 76% and sinuate, 15.37%.

Two types dominate the rondels (97.33%): Towers, 63.33% and rondels *sensu stricto*, 34%. Lastly, for the lobate class, 86.33% of the variability is represented by small bilobates with concave ends (61.58%), small bilobates with flat ends (16.04%), and small bilobates with convex ends (8.34%). Four lobate types were found exclusively in soils: small bilobate with notched ends, large bilobate with flat ends, large bilobate with notched ends, and cross. The saddle class is uncommon (5.87%) and the short saddle dominates it (74.32% of the subtotal), while squat saddles are rare. Generic tabulars (3.88% of the total), bulliforms and lanceolates (2.89% of the total), generic cylindrical phytoliths (1.23% of the total), sclereids (1.1% of the total), fusiforms / gutiforms (0.74% of the total) (nomenclature not per ICPN 1.0), and clavates (0.25% of the total) are scarce. The remainder includes composite epidermal tissue, polygonal prisms with subrounded top (cf. *Commelinaceae*), and papillae; and they all are extremely uncommon.

Soils also produced 1,564 diatoms in addition to the phytolith complement summarized above. The mean number of diatoms per sample is 44.68 and the median recovery is 9.50 with a range of zero –301. The specimens are mostly from the Nitzschoid group (Figs. 4af–4ah), which grows in wet soils. The diatom count per plant cover class is inversely

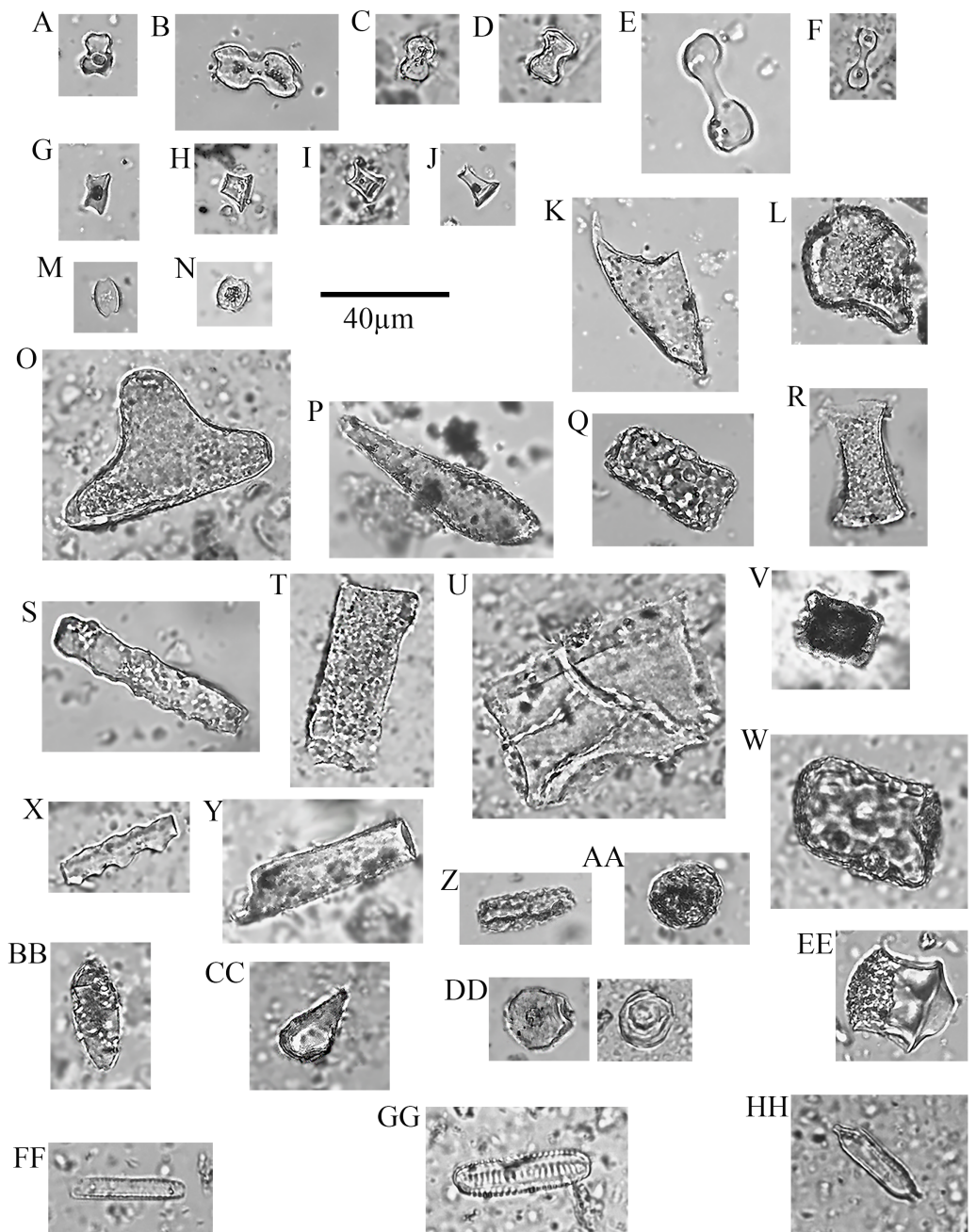


Figure 4 Soil phytoliths and diatoms. (A) bilobate, short concave (#30); (B) bilobate, short notched (#166); (C) bilobate short convex (#54); (D) bilobate, short flat (#112); (E) bilobate, long concave (#145); (F) bilobate, long convex (#98); (G) rondel (#30); (H) tower (#112); (I) tower, horned (#112); (J) tower, tapered (#65); (K) lanceolate (#30); (L) bulliform (#54); (M) saddle, squat (#30); (N) saddle (#65); (O) sclereid (#191); (P) clavate (#65); (Q) tabular thick lacunate (#54); (R) tabular strangulated (#127); (S) tabular sinuate (#120); (T) tabular scrobiculate (#65); (U) tabular sulcate (#30); (V) blocky (#30); (W) blocky thick lacunate (#2); (X) cylindroid sinuate (#65); (Y) cylindroid scrobiculate (#149); (Z) cylindroid thick lacunate (#30); (AA) globular granulate (#191); (BB) guttiform (#30); (CC) fusiform (#54); (DD) globular facetate (#30); (EE) polygonal prism (#131); (FF–HH) diatoms (#65, 112, 258).

Full-size [DOI: 10.7717/peerj.8211/fig-4](https://doi.org/10.7717/peerj.8211/fig-4)

Table 2 Topsoil phytolith counts per group, class, and morphotype.

Major group	Phytolith class	Phytolith morphotype	Count		
Poaceae short cell	Lobate	Bilobate, long concave	38		
		Bilobate, long convex	8		
		Bilobate, long flat	14		
		Bilobate, long notched	4		
		Bilobate, short concave	428		
		Bilobate, short convex	58		
		Bilobate, short flat	114		
		Bilobate, short notched	28		
	Rondel	Cross	Cross	1	
			Polylobate	2	
		Rondel, horned	Rondel, horned	8	
			Rondel, truncated	12	
			Rondel, tower	475	
		Rondel	Rondel	255	
			Saddle, ovate	24	
			Saddle, short	469	
		Saddle	Saddle, squat	140	
			Blocky	879	
		Blocky	Blocky corniculate	Blocky corniculate	2
				Blocky ridged	405
	Blocky scrobiculate		Blocky scrobiculate	23	
			Blocky sinuate	28	
	Blocky thick lacunate		Blocky thick lacunate	72	
			Cylinder corniculate	3	
	Cylindrical	Cylinder psilate	Cylinder psilate	132	
			Cylinder scrobiculate	569	
		Cylinder sinuate	Cylinder sinuate	115	
			Cylinder thick lacunate	61	
	Fusiform	Fusiform	11		
		Guttiform	68		
	Sclereid/Clavate	Clavate	27		
		Sclereid	119		
Woody	Globular bisected	Globular bisected	1		
		Globular facetate	778		
	Globular granulate	Globular granulate	83		
		Globular granulate, large	3		
	Spherical	Globular granulate oblong	24		
		Globular psilate	10		
	Globulose	Globulose	2		
		Globulose segmented	1		
	Oblong granulate	Oblong granulate	10		
		Hemisphere psilate	3		

(continued on next page)

Table 2 (continued)

Major group	Phytolith class	Phytolith morphotype	Count
		Tabular corniculate	11
		Tabular ellipsoidal	35
		Tabular ellipsoidal, large	21
		Tabular facetate	8
		Tabular laminate	186
	Tabular	Tabular oblong	16
		Tabular pilate	3
		Tabular scrobiculate	2036
		Tabular sinuate	918
		Tabular strangulated	11
		Tabular sulcate	509
		Tabular thick lacunate	731
Undetermined grass	Grass, undetermined	Bulliform	47
		Trichome	264
	Composite	Epidermal	3
		Vessel	18
	Drum	Polygonal prism	2
Rare/Unknown	Sedge	Papillae	1
	Short cell, other	Trapeziform sinuate	1
	Tabular	Tabular	70
	undetermined	Tabular crenate	36
		Tabular psilate	311

proportional to density of plant cover today, with the highest frequency in soil samples without vegetation and/or sparse growth probably because of pooling water in these areas (Albert, Bamford & Cabanes, 2006).

Extraction weight and plant cover

Conventionally, extraction weights are reported as a proxy of phytolith concentration. Like others before us (Blinnikov, Bagent & Reyerson, 2013), however, we did not see a discernible pattern between plant cover, phytolith count, and extraction weight (Fig. S1) with values randomly distributed. Thus, plant cover rank zero varied between 43.6%–69.5%, for rank one between 40.96%–70.77%, rank two between 25.23%–63.56%, and rank three between 41.1%–56.16%. The scores for plant cover ranks overlap, and so do those for extraction weight versus terrain elevation.

We explored the relationships between plant cover rank and phytoliths from woody dicots versus grasses. The woody phytolith group dominates all terrain ranks, and appears to increase with denser plant cover, while grass phytoliths peak in sparsely vegetated terrain. The null hypothesis posits that if plant cover has no influence on the relative proportions of woody and grass phytoliths, there will be no significant difference between overall proportions and plant cover rank proportions. For plant cover rank zero, vegetation density has not significantly influenced the relative proportions of woody and grass phytoliths present in the topsoil (Chi-square = 2.382, not significant at $p < 0.10$). There

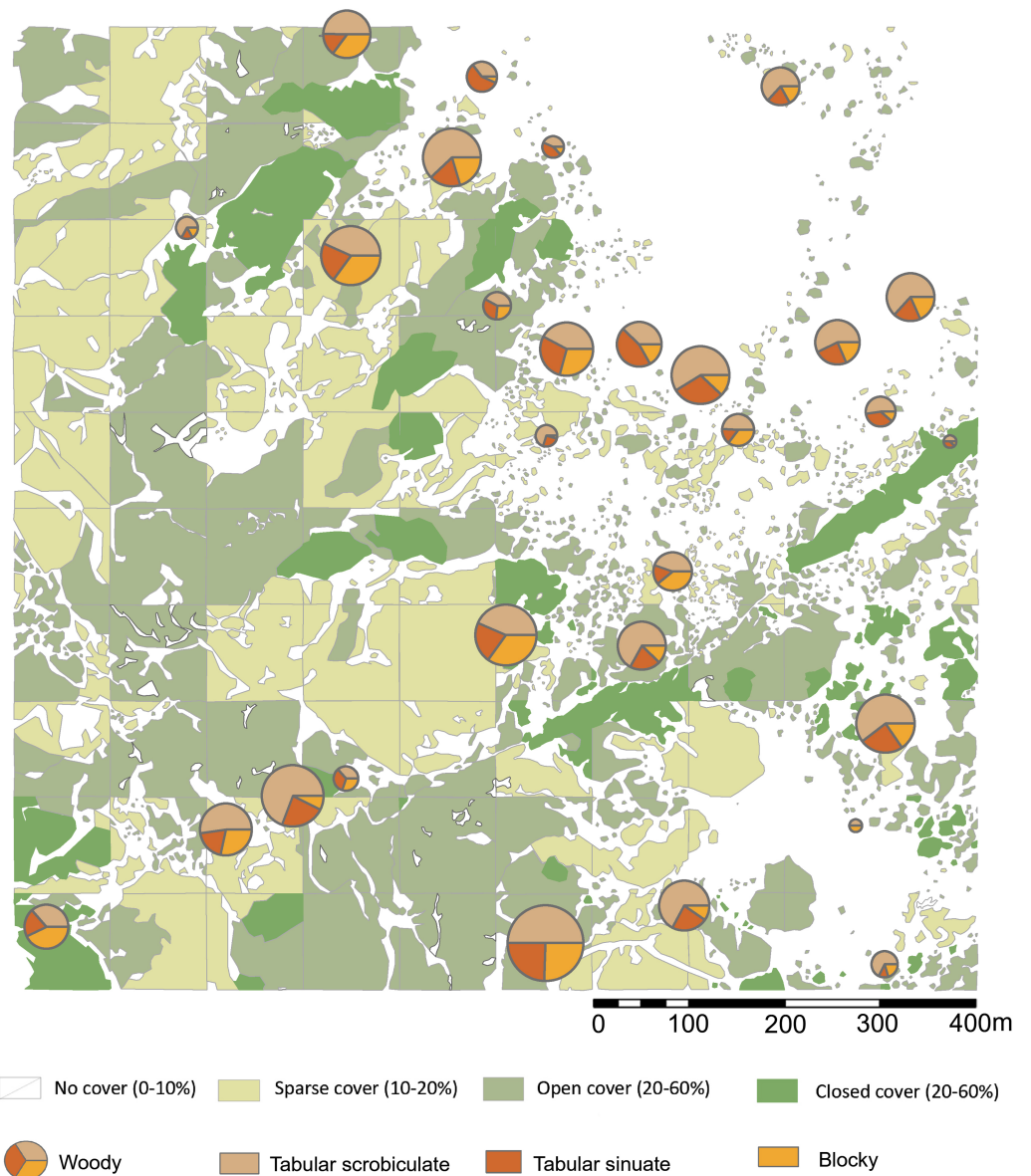


Figure 5 Highest ranking woody phytolith proportions in relation to plant cover rank. Please see Figs. 1 and 2 for location of sampling area and corresponding sample numbers. Digitized 2017 ESRI ArcGIS.

Full-size DOI: [10.7717/peerj.8211/fig-5](https://doi.org/10.7717/peerj.8211/fig-5)

are significant differences in all other plant landscapes: Rank one has significantly more grass phytoliths than expected from the null hypothesis (Chi-square = 9.0812, $p < 0.01$) while ranks two (Chi-square = 7.2288, $p < 0.01$) and three (Chi-square = 8.0625, $p < 0.01$) have many more woody phytoliths. Statistically, therefore, sparse, open, and closed terrain influenced the relative proportions of woody and grass phytoliths released into the soil (Table 3), with sparse land containing more grass phytoliths, and open woodland / closed terrain supporting more woody dicot types.

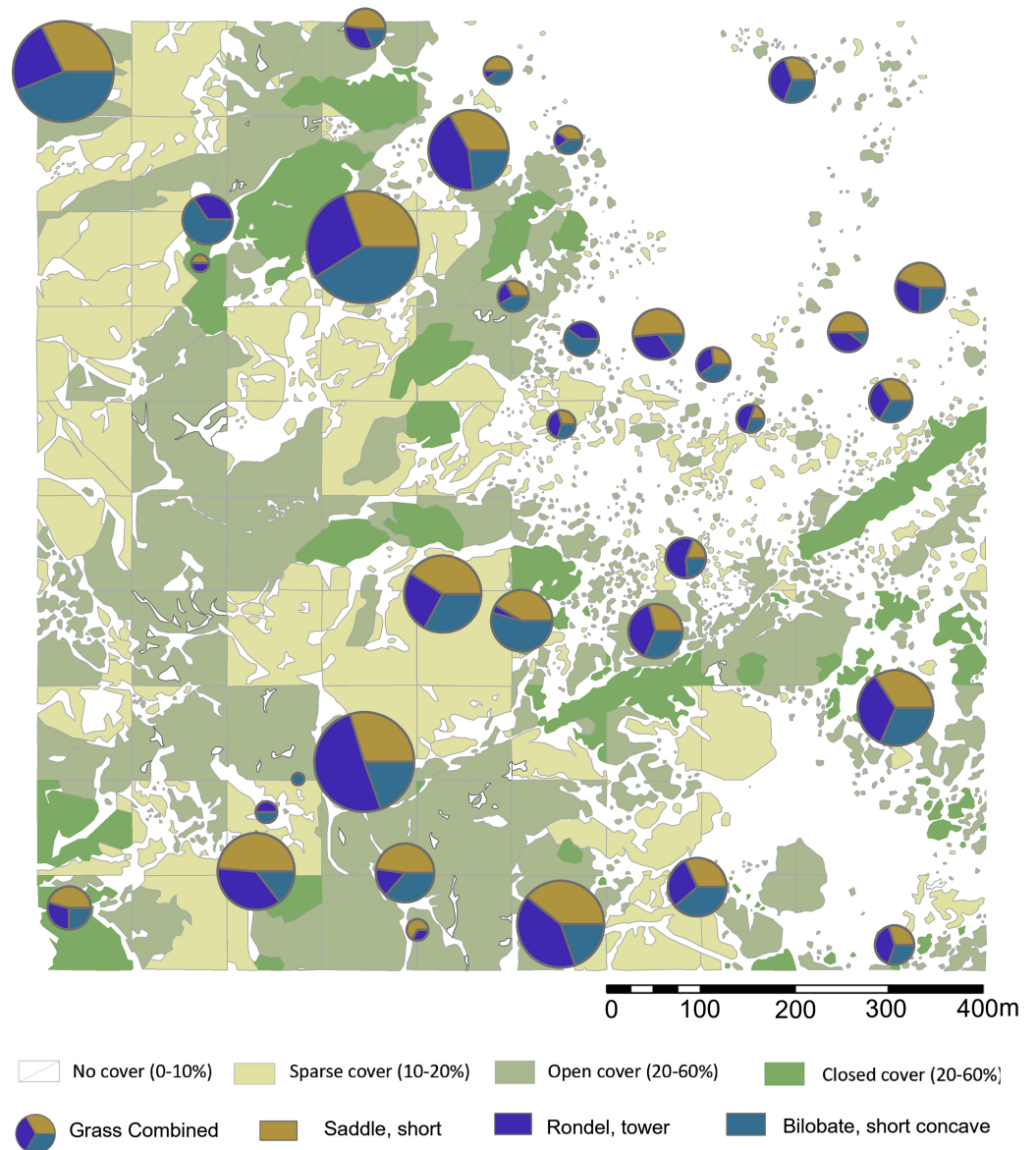


Figure 6 Highest ranking short cell phytolith proportions in relation to plant cover rank. Digitized 2017 ESRI ArcGIS. Please see Figs. 1 and 2 for location of sampling area and corresponding sample numbers. Digitalized Source: Google Maps.

Full-size DOI: [10.7717/peerj.8211/fig-6](https://doi.org/10.7717/peerj.8211/fig-6)

For short cell classes (Table 4), rank zero yields rondels followed by lobates and saddles; rank one: lobates, saddles, and rondels; rank two and three: lobates, rondels, and saddles. These class fluctuations across plant cover, however, are artifacts of differing sample numbers per plant zone (Figs. S2–S4). Chi-square testing revealed no significant changes in short cell class related to plant cover rank. By morphotype, the most frequent phytoliths are towers, short saddles, and small bilobates with concave ends. In ranks zero and one, this order is preserved, but it reverses in ranks two and three. That is, the tandem of towers and short saddles are more frequent in areas of sparse to no plant cover (rank zero, one), while

Table 3 Woody versus grassy phytoliths per plant cover rank, and short cell breakdown in topsoils.

Plant cover rank	Woody	Grass	Short cell class Lobate	Rondel	Saddle	Grand total
0	74.8	25.2	34.4	36.3	29.3	100.0
1	72.7	27.3	29.0	39.3	31.7	100.0
2	79.3	20.7	35.8	33.3	30.9	100.0
3	80.8	19.2	37.3	33.3	29.4	100.0

short saddles and small bilobates with concave ends are more frequent in areas of increased plant cover (rank two, three). However, Chi-square testing shows no significant change in the relative frequencies of short cell morphotypes related to plant cover today. In fact, where one phytolith type increases in frequency, so do the other two: These morphotypes vary positively with each other.

Plant phytoliths

Production

All plant samples contained phytoliths, except for the woody tissue of *Commiphora kua*. A total of 4,310 phytoliths were classified (Tables 5, 6) in morphotypes ($n = 52$) and classes ($n = 13$). The median number of phytoliths per species is 130 (range: zero –539) and were found mostly in leaf material (62.01%) with specimens from woody tissue making up the second largest group (23.52%) (Fig. 7, Table S1). The number of samples from leaf and woody tissue was identical at nineteen each. Leaf samples produced on average two and a half times as many phytoliths, with the exception of *Balanites aegyptiaca*, *Melhaniania parviflora*, and *Ocimum* spp. in which woody tissue generates more phytoliths. Where extraction weights of phytoliths can be compared between leaf and woody tissue from the same species ($n = 13$), leaf samples have a slight tendency to produce larger extraction percentages (8/13).

We do not see a correlation between high phytolith production and the number of morphotypes per taxon (Table 7). The average yield per morphotype is 83 phytoliths. Three types top the highest frequency with figures six times higher than the average: oblong granulate, small bilobate with concave ends, and rondel ovate. In second place, tabular, globulose, vessels, and short saddles. Average richness is noticed for tabular psilate, globular granulates, epidermal cells, hair complex phytoliths, mesophyll cells, and large bilobates with convex ends. Also included in this group are rondel tower, rondel horned, and blocky. All other morphotypes appear at below average frequency. Thus, highly polymorphic species generate average phytolith amounts, and low polymorphic taxa can be top silica accumulators; however, all but one species among the poor phytolith producers (*Balanites aegyptiaca*) fall within the low polymorphism group, probably an artifact of small sample size.

Richness

Five taxonomic groups can be distinguished:

1. Top producers rank at median values almost three times higher than the rest of the group (~332 phytoliths per mount). The lead type is *Boscia angustifolia* (Capparaceae),

Table 4 Percent of short cell morphotypes per plant cover rank in topsoils.

Morphotype	Plant cover rank				Grand total
	0	1	2	3	
Most frequent short cell					
Rondel, tower	36.7	36.9	30.6	31.9	34.6
Saddle, short	33.5	34.1	35.8	32.6	34.2
Bilobate, short concave	29.9	29.0	33.6	35.4	31.2
Grand total	100.0	100.0	100.0	100.0	100.0
Saddle					
Saddle, ovate	10.4	0.0	0.6	0.0	3.8
Saddle, short	70.7	71.8	80.2	79.7	74.3
Saddle, squat	18.9	28.2	19.6	21.7	22.1
Grand Total	100.0	100.0	100.0	100.0	100.0
Rondel					
Rondel, horned	1.9	0.9	0.6	0.0	1.1
Rondel, tower	62.5	62.6	63.4	68.7	63.3
Rondel, truncated	2.5	0.9	1.1	1.5	1.6
Rondel	33.1	35.6	34.9	29.9	34.0
Grand Total	100.0	100.0	100.0	100.0	100.0
Bilobate					
Bilobate, long concave	5.4	4.7	5.9	6.7	5.5
Bilobate, long convex	1.9	0.6	1.1	0.0	1.2
Bilobate, long flat	3.5	1.2	1.1	1.3	2.0
Bilobate, long notched	1.5	0.0	0.0	0.0	0.6
Bilobate, short concave	53.8	66.9	64.9	68.0	61.6
Bilobate, short convex	8.1	7.6	9.0	9.3	8.3
Bilobate, short flat	21.5	16.3	11.2	12.0	16.4
Bilobate, short notched	3.8	1.7	6.9	2.7	4.0
Cross	0.0	0.6	0.0	0.0	0.1
Polylobate	0.4	0.6	0.0	0.0	0.3
Grand Total	100.0	100.0	100.0	100.0	100.0

along with three members of the Poaceae representing three subfamilies, Panicoideae, Chloridoideae, and Aristidoideae. In this area, grassy species produce many more phytoliths than most other plants, outproducing other functional classes by factors ranging between 1.63 and 27.83.

- High values are also reported for a group of five species with median phytolith number of 218. Four of these species belong with the Chloridoid grasses. One member is with the Olacaceae (*Ximения caffra*).
- Average production was noticed in two members of the genus *Acacia* (*tortilis*, *nilotica*) (Fabaceae). Other notable producers include *Melhanía* (Malvaceae), *Maerua* (Capparaceae), *Cissus* (Euphorbiaceae), and *Barleria* (Acanthaceae).

Table 5 Plant phytolith counts per group, class, and morphotype.

Major group	Phytolith class	Phytolith morphotype	Count	
Poaceae short cell	Lobate	Bilobate, long concave	26	
		Bilobate, long convex	102	
		Bilobate, short concave	491	
		Bilobate, short convex	30	
		Bilobate, short flat	19	
	Rondel	Rondel	Polylobate	19
			Rondel, horned	82
			Rondel, ovate	464
		Saddle	Rondel, tower	86
			Rondel	11
		Blocky	Saddle, short	211
			Saddle, squat	15
		Cylindrical	Blocky	79
			Blocky radiating	9
			Blocky scrobiculate	1
		Fusiform	Cylinder crenate	8
	Cylinder psilate		35	
	Sclereid/Clavate	Cylinder scrobiculate	6	
		Cylinder sinuate	46	
	Woody	Spherical	Fusiform	16
			Guttiform	23
		Tabular	Clavate	7
			Sclereid	11
			Globular granulate	132
			Globular granulate, large	2
			Globular granulate oblong	11
Globular psilate			1	
Globular tuberculate			5	
Globulose			239	
Hemisphere psilate			1	
Oblong granulate			596	
Tabular ellipsoidal			46	
Tabular laminate			4	
Tabular oblong			9	
Tabular scrobiculate	113			
Tabular sinuate	74			
Tabular strangulated	2			
Tabular subrounded	18			
Tabular sulcate	3			
Tabular thick lacunate	12			

(continued on next page)

Table 5 (continued)

Major group	Phytolith class	Phytolith morphotype	Count
Undetermined grass	Grass, undetermined	Bulliform	63
		Trichome	19
	Composite	Epidermal cells	131
		Vessel	224
		Globular mesophyll	127
		Hair	62
Rare/Unknown	Epidermal complex	Hair base	104
		Palisade	6
		Stomata	17
	Tabular, undetermined	Tabular	279
		Tabular crenate	54
		Tabular psilate	159

- Low producers with a median of 104 phytoliths include *Ocimum* (Lamiaceae) and *Commiphora* (Burseraceae), and members of the Acanthaceae, Asphodelaceae, and Asparagaceae.
- Very poor phytolith producers (median value = 19) comprise some of the most characteristic taxa in the region; namely, *Acacia mellifera*, *Balanites aegyptiaca*, three *Commiphora* species, the most emblematic taxon of Oldupai Gorge (*Sansevieria robusta*), *Salvadora persica*, and the genus *Sarcostemma* (Apocynaceae): The lowest absolute rank in the region is that of *Sarcostemma viminale*.

Morphotypes

The morphotypes from woody plants are led by the globular class through three phytoliths: Oblong shapes with a granulate texture, globulose, and globular granulate. The tabular class includes three morphotypes in abundance: scrobiculate, sinuate, and ellipsoidal; while the cylindrical class peaks with cylinder sinuates and psilates. Blocky morphotypes are relatively common, but four blocky morphotypes could not be found in the local plants we studied: corniculate, ridged, sinuate, and thick lacunate. The Poaceae produce various rondel types, dominated by ovates, towers, and horned towers. Lobate phytoliths comprise six variants but are mostly manifested through two types: small bilobates with concave ends (e.g., Panicoid type) and large bilobates with convex ends (e.g., Aristidoid type). The saddle class comprises two types largely dominated by short saddles both being very common in *Cynodon dactylon*. Several cylindrical phytoliths were documented in thirteen local dicots but were absent or extremely infrequent among the Poaceae: cylindrical crenate, psilate, scrobiculate, and sinuate.

DISCUSSION

The Acacia-Commiphora Analog

In East Africa, the transition to arid-adapted woodlands and grasslands over the last two million years has been documented in pedogenic carbonates (Cerling, Bowman & O'Neil, 1988; Levin et al., 2004; Levin et al., 2011; Quinn et al., 2007), mammal, bird, and fish fossils

Table 6 Count of phytoliths by species and major group in descending order.

Species	Phytolith major group				Grand total
	Poaceae short cell	Rare/Unknown	Undetermined grass	Woody	
<i>Boscia angustifolia</i>	0	2	0	537	539
<i>Pennisetum mezianum</i>	264	64	6	0	334
<i>Sporobolus africanus</i>	302	16	12	0	330
<i>Aristida adoensis</i>	186	78	15	1	280
<i>Sporobolus consimilis</i>	192	2	43	0	237
<i>Sporobolus spp.</i>	207	20	0	0	227
<i>Cynodon dactylon</i>	208	6	5	0	219
<i>Sporobolus panicoides</i>	197	19	1	0	217
<i>Ximenia caffra</i>	0	183	0	22	205
<i>Melhanian parviflora</i>	0	61	0	122	183
<i>Acacia tortilis</i>	0	94	0	75	169
<i>Maerua tryphilla</i>	0	66	0	102	168
<i>Acacia nilotica</i>	0	96	0	64	160
<i>Cissus cactiformis</i>	0	59	0	81	140
<i>Barleria eranthemoides</i>	0	85	0	45	130
<i>Ocimum spp.</i>	0	33	0	89	122
<i>Commiphora spp.</i>	0	121	0	0	121
<i>Hypoestes forskalii</i>	0	2	0	107	109
<i>Aloe secundiflora</i>	0	3	0	97	100
<i>Asparagus africanus</i>	0	54	0	24	78
<i>Acacia mellifera</i>	0	12	0	45	57
<i>Balanites aegyptiaca</i>	0	23	0	34	57
<i>Commiphora africana</i>	0	4	0	25	29
<i>Cissus quadrangularis</i>	0	21	0	4	25
<i>Commiphora merkeri</i>	0	10	0	13	23
<i>Sansevieria robusta</i>	0	13	0	10	23
<i>Salvadora persica</i>	0	10	0	6	16
<i>Sarcostemma viminalis</i>	0	6	0	6	12
Grand Total	1556	1163	82	1509	4310

([Bibi & Kiessling, 2015](#); [Bibi et al., 2018](#); [Prassack et al., 2018](#)), micro- and macrobotanical remains like pollen, phytoliths, and wood ([Bonnefille, 1982](#); [Bonnefille, 1995](#); [Barboni et al., 1999](#)), and stable isotopes of hydrogen and carbon from leaf wax lipid biomarkers ([Magill, Ashley & Freeman, 2013a](#); [Magill, Ashley & Freeman, 2013b](#); [Uno, Polissar & Jackson, 2016](#); [Lupien et al., 2018](#)).

The phytoliths from present-day vegetation and soil surfaces are the baseline to interpret palaeolandscapes and ecological niches that might have been occupied by early hominins. To study the influence of plant community structure and cover on human ecology, soil phytolith assemblages under known vegetation density and composition can provide a referential to interpret key palaeoecological aspects of early Pleistocene floristic regions and their main vegetation types.

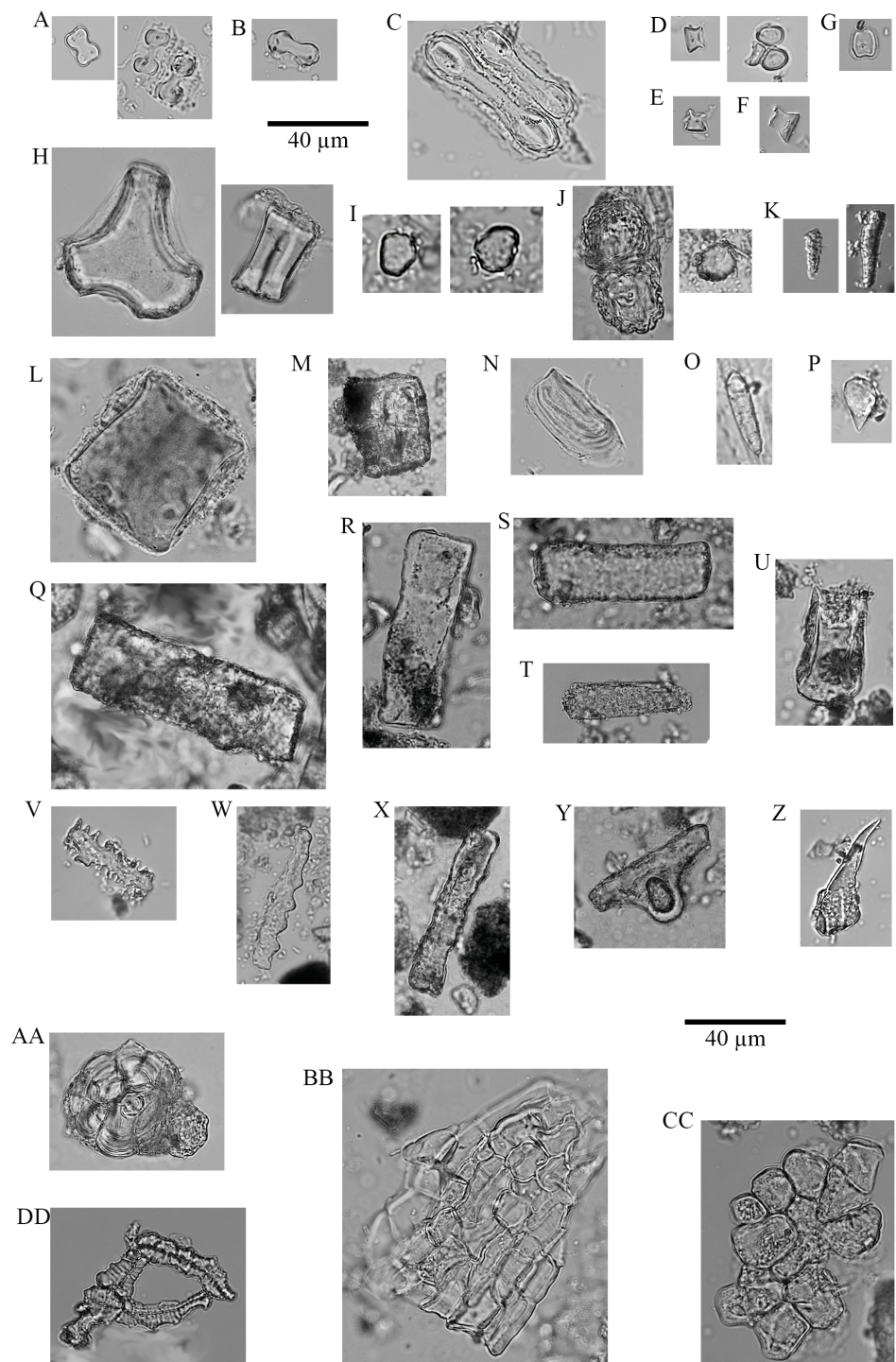



Figure 7 Plant phytoliths. (A) bilobate, short concave (left: *P. mezialum* right: *A. adoensis*); (B) bilobate, short convex (*A. adoensis*); (C) bilobate, long convex (*A. adoensis*); (D) rondel, ovate (*S. panicoides*); (E) rondel, horned (*S. spp.*); (F) tower (*S. consimilis*); (G) saddle, short (*C. dactylon*); (H) bulliform (*S. consimilis*); (I) globulose (*A. secundiflora*); (J) globular granulate (continued on next page...) Full-size  DOI: 10.7717/peerj.8211/fig-7

Figure 7 (...continued)

(left: *B. eranthemoides* right: *A. secundiflora*); (K) oblong granulate (left: *B. angustifolia*; right: *H. forskoolii*); (L) blocky (*Ocimum spp.*); (M) blocky (*A. tortilis*); (N) blocky radiating (*X. caffra*); (O) fusiform (*O. spp.*); (P) guttiform (*C. cactiformis*); (Q) tabular sinuate (*A. mellifera*); (R) tabular psilate (*A. mellifera*); (S) tabular (*A. tortilis*); (T) tabular scrobiculate (*M. tryphilla*); (U) tabular strangulated (*S. persica*); (V) tabular crenate (*S. consimilis*); (W) cylinder sinuate (*A. nilotica*); (X) cylinder scrobiculate (*C. cactiformis*); (Y) sclereid (*A. tortilis*); (Z) hair (*C. dactylon*); (AA) hair base (*X. caffra*) (BB) epidermal cells (*B. eranthemoides*); (CC) globular mesophyll (*X. caffra*); (DD) vessel (*A. tortilis*).

Table 7 Plant species studied for phytolith reference, with polymorphism per taxon.

Clade (Poaceae)	Species	Morphotype, n
	<i>Aloe secundiflora</i>	8
	<i>Acacia mellifera</i>	9
	<i>Acacia nilotica</i>	11
	<i>Acacia tortilis</i>	20
Aristidoideae	<i>Aristida adoensis</i>	15
	<i>Asparagus africanus</i>	7
	<i>Balanites aegyptiaca</i>	15
	<i>Barleria eranthemoides</i>	15
	<i>Boscia angustiflora</i>	3
	<i>Cissus cactiformis</i>	14
	<i>Cissus quadrangularis</i>	6
	<i>Commiphora africana</i>	8
	<i>Commiphora merkeri</i>	6
	<i>Commiphora kua</i>	0
	<i>Commiphora spp.</i>	6
Chloridoideae	<i>Cynodon dactylon</i>	5
	<i>Hypoestes forskoolii</i>	6
	<i>Maerua triphylla</i>	11
	<i>Melhanian parviflora</i>	15
	<i>Ocimum spp.</i>	16
Panicoideae	<i>Pennisetum mezianum</i>	7
	<i>Salvadora persica</i>	6
	<i>Sansevieria robusta</i>	7
	<i>Sarcostemma viminalis</i>	5
Chloridoideae	<i>Sporobolus africanus</i>	10
Chloridoideae	<i>Sporobolus consimilis</i>	8
Chloridoideae	<i>Sporobolus panicoides</i>	4
Chloridoideae	<i>Sporobolus spp.</i>	6
	<i>Ximania caffra</i>	14

We provide a phytolith analog for *Acacia-Commiphora* mosaics that may represent the trend for more open landscapes recorded in East Africa since the early Pleistocene. In this analog, the cohort of phytolith morphologies that identifies semiarid woodland include tabular scrobiculate, tabular sinuate, blocky, globular facetate, tabular thick lacunate, cylinder scrobiculate, tabular sulcate, tower, short saddle, small bilobate with concave

ends, and blocky ridged. We did not find unique identifiers or highly diagnostic shapes for the most typical species that today make up the *Acacia-Commiphora* ecosystem, but this is hardly surprising and confirms similar observations in adjacent regional centers of plant endemism, such as the Zambezi woodland, where woody dicot types have very little taxonomic power (Mercader *et al.*, 2009) because of redundancy across orders (Bozarth, 1992). Also in common with phytolith spectra from plants and soils in Zambezi woodlands (Mercader *et al.*, 2009; Mercader *et al.*, 2010; Mercader *et al.*, 2011), there is severe overrepresentation of robust morphotypes such as tabulars, blockies, and globulars in addition to lobate short cells.

Do soil phytoliths mirror physiognomy and composition of vegetation aboveground?

We address this question at two levels, regional (plot = 100 ha) and local (quadrat = 6.25 ha). When considering the larger regional plot, all soil samples are dominated by phytoliths from woody dicots (Table S2–S4) (Albert, Bamford & Cabanes, 2006):

The blocky morphotypes that could not be found in local plants (corniculate, ridged, sinuate, and thick lacunate) were partly tracked by geo-referencing: Blocky ridged and thick lacunate associate with areas of sparse plant growth (Figs. S5–S6). Large numbers of these forms in soils suggest that plants not represented in our inventory might have produced them or that the species producing these types have disappeared in past decades or not seasonally available when we collected our samples.

Cylindrical phytoliths were common in many of the local but were either absent or extremely infrequent among the grasses. Cylinder corniculates and thick lacunates occur only in the soils, while crenates occur only in plants. Cylinder crenates appear in *Acacia mellifera* and *Ocimum* spp. Similarly, the few corniculates recovered from soils may not be inferentially important. However, the relatively large number of cylinder thick lacunates in soils is noteworthy, as plants from the Miombo woodlands (Mercader *et al.*, 2009) produce them. Fusiforms, guttiforms, clavates, and sclereids are found in plants and soils.

The globular class is common in both soil and plant samples. The globular facetate (mesophyll cells) is very abundant, and geo-referencing shows an association with areas covered by plants and absence from bare places (Fig. S7). Two globulose morphotypes were recovered from soils only: globulose bisected and segmented. The former is a unique phytolith that, in adjacent Zambezi woodlands, is restricted to the Solanaceae (Mercader *et al.*, 2009: Fig. 3AE).

Tabular phytoliths are relatively uncommon in the plants but very common in the soils. Four morphotypes could not be found amongst the plants, but were in soil samples: corniculate, ellipsoidal large, facetate, and pilate. Their georeferencing shows no pattern for three of them, but one type (tabular ellipsoidal large) appears solely in locations with plants growing today.

Poaceae phytoliths are skewed in their soil expression (Table 8, Table S5): the local grasses are demonstrated overproducers (Twiss, Suess & Smith, 1969; Novello *et al.*, 2012) but they are not overrepresented in these soils, rather the opposite. We infer that topsoils embody plant communities, past and present, in a time-averaged palimpsest dominated

Table 8 Topsoil and plant phytolith counts per group and class within the 6.25 ha catchment transect.

Major group	Phytolith class	Plants $n = 18$	Topsoil $n = 6$
Poaceae short cell	Lobate	169	60
	Rondel	197	61
	Saddle	225	78
	Blocky	69	290
	Cylindrical	65	80
Woody	Fusiform	30	21
	Sclereid/Clavate	11	15
	Spherical	185	59
	Tabular	166	1087
Undetermined grass	Grass, undetermined	21	65
	Composite	195	2
Rare/Unknown	Epidermal complex	201	0
	Tabular, undetermined	263	94

by woodlands (Table S3). It is likely that the heterogenous landscape and the changing grazing history, erosion, and fire regime by pastoralists over the last 60 years (Sinclair *et al.*, 2008) have created a phytolith record of ecological succession underscored by a reversion towards a dominance of woody vegetation, as independently recorded by studies of land cover change (Sinclair *et al.*, 2007; Niboye, 2010) that denote a low human impact on ecosystem dynamics since the 1960s.

Within the short cells, three major classes were identified in plants and soils: lobates, rondels, and saddles; albeit saddles are overrepresented in soils. Ten phytolith morphotypes were recovered within the lobate class. Of these, six were found in both plant and soil samples and four were found only in soils (small bilobate with notched ends; large bilobate with flat ends; large bilobate with notched ends; cross). The lead lobate type (Fahmy, 2008; Neumann *et al.*, 2017), small bilobate with concave ends, is produced abundantly in one local and one regional taxon: *Pennisetum mezianum* and *Sporobolus africanus* respectively. Aristidoid, large bilobates with convex ends are documented in *Aristida adoensis* while small bilobates with flat ends appear in *Pennisetum mezianum*. Rondel class phytoliths are common in both plants (*Sporobolus* specimens) and soils. Rondel ovates are unique to the plant sample, while truncated rondels occur only in soils. Rondels and horned rondels appear in *Sporobolus* spp. The absence of rondel ovates in the soils is notable given their preponderance in the genus *Sporobolus*. Saddles were recovered from three plants. Saddle squats are present in *Cynodon dactylon* and the abundance of this morphotype in the soil samples may suggest correlation. Short saddles are found in plants and soils while saddle ovates are from soils but not plants. In brief, short cell phytoliths from soils do not always reflect the grass species growing in them today.

Catchment

We explore the notion of catchment by zooming into one local quadrat covering 6.25 ha to conduct a side-by-side comparison of phytolith assemblages from topsoils ($n = 6$) and plants ($n = 18$) (Table 8, Tables S4–S5). To do this, we tallied all phytoliths by class.

Of the thirteen phytolith classes represented in this quadrat, eight classes are severely underrepresented in the soil, including all three Poaceae short cell classes, two woody classes (globular/fusiform), epidermal cells in anatomical connection, and vessels (Bamford, Albert & Cabanes, 2006). Specifically, a positive balance exists for cylindrical shapes from woody tissue, along with sclereids and clavates. Moreover, dicot tabular morphotypes are overrepresented in the soil by a factor of seven. Several blocky morphotypes from woody tissue are four times more common in soils than in the plants that produced them, and lack of correspondence was similarly noticed for bulliforms and lanceolates. We attribute this imbalance to the phytolith signal from grasses being dampened by an overwhelming accumulation of woody phytoliths.

Rich phytolith producers such as the Poaceae display differential representation in soils, especially at sampling loci where they were growing. For instance, *Cynodon dactylon* produces short and squat saddles. In the quadrat where it grows today the average frequency of short saddles is half ($n = 7.5$) of the local average ($n = 13$), and the same applies to squat saddles (this quadrat = 1.8 versus 3.5 in the rest of the collection). *Sporobolus panicoides* preferentially generates rondel ovates, but none could be found in any of the six soil samples surrounding it. *Aristida adoensis* supports a majority of large bilobates with convex edges, and the average representation in the plant ($n = 0.2$) is similar to that in the soils nearby ($n = 0.3$). Importantly, one of the highest ranked short cells from both collections, soils and plants, the small bilobate with concave ends, attains lower than average representation in the soils under scrutiny ($n = 4.8/6$) perhaps because the main producers of this morphotype (*Pennisetum mezianum*, *Sporobolus africanus*) were not close.

Considering that all phytolith classes found in the living tissues of the eighteen plant taxa growing within this quadrat are recorded in the underlying soil surface it can be suggested that the catchment area for these soil phytolith assemblages is smaller than five hectares (Blinnikov, 1994; Fredlund & Tieszen, 1994; Blinnikov, Busacca & Whitlock, 2002).

Ecological disturbance, time averaging, heterogeneity, and sampling methods

The soil and plant phytolith assemblages are clearly distinguishable from one another. The presence of rare group phytoliths influences ratios in plants (26.98% of the total assemblage) and is much less an aspect of the soils (4.11%). However, even if we were to remove rare and delicate morphotypes, and consider short cells and woody dicot phytoliths only, the differences between the two datasets are obvious. In the plants, the two major groups are near parity (ratio = 1.031; Poaceae $n = 1,556$ / woody $n = 1,509$) while in the soils the two groups are quite disparate in relative frequency (ratio = 0.263; Poaceae $n = 1,509$ and woody $n = 7,914$).

Soil samples are not homogenous relative to one another. We indicated statistically significant relationships between the soil phytolith population in samples collected under a given plant cover and the rank of that zone, although not all individual samples show this relationship. The ratio between Poaceae short cells and woody phytoliths varies widely from 1:1 to 0:1. Moreover, soil samples with high number of Poaceae short cells have the highest number of woody phytoliths. Even in the most open parts of the landscape

phytoliths from woody tissue outnumber those from grasses (*Gao et al., 2018a; Gao et al., 2018b*) and some woody types abound in soils but are absent from the local plants sampled (*Albert, Bamford & Esteban, 2015*).

We are suggesting decadal inheritance of soil phytoliths, as evidenced by:

- 1) The highest phytolith recovery is from areas without plant cover or Rank Zero.
- 2) No significant change in the relative frequencies of short cell morphotypes related to plant cover today.
- 3) Multiplicity of soil phytolith types, woody and grassy, that cannot be traced back to local plants.
- 4) Several phytolith classes are overrepresented in the soils.

That is, although soil phytoliths might represent 'decay-in-place' (*Piperno, 2006*), as well as transport by wind, water, fire and herbivory (*Fredlund, Egan & Howell, 2001*), the two phytolith populations reported here, from plants and soils, will always differ from each other because soil assemblages are the sum of phytolith accumulations and losses over time (*Fredlund & Tieszen, 1994; Kerns, Moore & Hart, 2001*).

CONCLUSION

Over the last few decades, different environmental proxies have been utilized in Africa to identify present-day ecosystems that could be used as referentials to frame the emergence of the genus *Homo* (*Cerling, Bowman & O'Neil, 1988; Barboni et al., 1999; Barboni et al., 2010; Quinn et al., 2007; Albert & Marean, 2012; Barboni, 2014; Esteban et al., 2017; Novello et al., 2018; Prassack et al., 2018*). One of these analogs is the *Acacia-Commiphora* biome, where we studied a phytolith reference collection of characteristic plants that aided in the taxonomic identification of phytoliths from the underlying soils. This article also studied the resolution of phytoliths from present-day surfaces along the *Acacia-Commiphora* landscape to reflect woody dicot versus grassy plant cover, detecting the shifting boundary between woodlands and grasslands accurately: sparsely vegetated areas supported a larger pool of grass phytoliths while terrain covered by woody taxa yielded more woody phytoliths. In addition, soil phytolith assemblages recorded decadal ecological succession and changes in vegetation communities.

The comparison of soil phytoliths with local plants suggested that differential production, accumulation, and preservation interplay at the soil level. Well-known silica accumulators such as grasses seem localized and minor because of the cyclical, long-term succession to woodland. Although grasses boomed and busted through the waxing and waning of anthropogenic disturbance by fire and grazing, the long-term accumulation of woody types counterbalanced Poaceae representation. Therefore, phytoliths from local soils are capable of identifying woodlands as the climactic land cover across the landscape and they have value as a long-term proxy to detect ecosystem change and regulation that become apparent over a period of decades. The areal catchment recorded in the soils of the eastern Serengeti Plains encompasses several hectares. Furthermore, a heterogeneous record calls for research design that is able to capture spatial variability, documented here through large-scale soil sampling. The identified phytolith analog will let future work

along the East African Rift System frame the environmental context of human evolution whenever the phytolith assemblages from associated sediments and paleosols yield a cohort of co-dominant types featuring the phytolith classes from dicot woody tissue and grasses identified here as typical of *Acacia-Commiphora* mosaics.

ACKNOWLEDGEMENTS

We thank the Tanzania Commission for Science and Technology, the Tanzanian Ministry of Natural Resources and Tourism (Division of Antiquities), the University of Dar es Salaam (DVC: Academic, Research), UDSM's College of Humanities and Department of Archaeology and Heritage, as well as the Oldupai Palaeoanthropology and Palaeoecology Project. We are grateful to the Tropical Pesticides Research Institute in Arusha. This work could not have been accomplished without the local Masai communities that welcomed us to their homeland and shared with us their expertise. A preprint of this manuscript has been made available online with the Open Science Framework (DOI <https://dx.doi.org/10.31219/osf.io/3ed7f>). We thank two anonymous reviewers and Dr. L. Wallis for their input.

ADDITIONAL INFORMATION AND DECLARATIONS

Funding

This work was supported by the Canadian Social Science and Humanities Research Council Partnership Grant 895-2016-1017. The funders had no role in study design, data collection and analysis, decision to publish, or preparation of the manuscript.

Grant Disclosures

The following grant information was disclosed by the authors:

Canadian Social Science and Humanities Research Council Partnership Grant: 895-2016-1017.

Competing Interests

Dale Walde is a member of the ASM Research Group. All authors declare that they have no competing interests.

Author Contributions

- Julio Mercader and Dale Walde conceived and designed the experiments, performed the experiments, analyzed the data, contributed reagents/materials/analysis tools, prepared figures and/or tables, authored or reviewed drafts of the paper, approved the final draft.
- Siobhan Clarke performed the experiments, analyzed the data, prepared figures and/or tables, authored or reviewed drafts of the paper, approved the final draft.
- Mariam Bundala, Jamie Inwood, Makarius Itambu, Fergus Larter, Patrick Lee and Aloyce Mwambwiga analyzed the data, prepared figures and/or tables, approved the final draft.
- Julien Favreau conceived and designed the experiments, performed the experiments, prepared figures and/or tables, approved the final draft.

- Garnet Lewiski-McQuaid and Laura Tucker performed the experiments, prepared figures and/or tables, approved the final draft.
- Neduvoto Mollel conceived and designed the experiments, contributed reagents/materials/analysis tools, prepared figures and/or tables, approved the final draft.
- Robert Patalano conceived and designed the experiments, prepared figures and/or tables, approved the final draft.
- Maria Soto performed the experiments, analyzed the data, contributed reagents/materials/analysis tools, prepared figures and/or tables, authored or reviewed drafts of the paper, approved the final draft.

Field Study Permissions

The following information was supplied relating to field study approvals (i.e., approving body and any reference numbers):

The Tanzania Commission for Science and Technology authorized this work under permit no. 2018-112-NA-2018-36. The Tanzanian Ministry of Natural Resources and Tourism, through its Antiquities Division, granted us permission to carry out this work (14/2017/2018) and authorities at the Ngorongoro Conservation Area allowed us to enter the protected area (BE.504/620/01/53). The export license for the materials presented in this study were obtained from the Antiquities Division (EA.150/297/01: 5/2018/2019) and the Tanzanian Executive Secretary from the Mining Commission (00001258).

Data Availability

The following information was supplied regarding data availability:

Detailed phytolith extraction protocols and full datasets with individual counts for both soils and plants are available at: Department of Anthropology & Archaeology, Tropical Archaeology Laboratory, "Protocols: extraction of phytoliths from modern plants and sediment, and preparation of sediment for particle size analysis," 2018, DOI <https://dx.doi.org/10.20383/101.0123>.

Mercader, Julio; Clarke, Siobhan; Bundala, Mariam; Favreau, Julien; Inwood, Jamie; Itambu, Makarius; Larter, Fergus; Lee, Patrick; Garnet Lewiski-McQuaid, Garnet; Mollel, Neduvoto; Mwambwiga, Aloyce; Patalano, Robert; Soto, Maria; Tucker, Laura; Walde, Dale, "Soil and Plant Phytoliths from the Acacia-Commiphora Mosaics at Olduvai Gorge (Tanzania)," 2018, DOI <https://dx.doi.org/10.20383/101.0122>.

Supplemental Information

Supplemental information for this article can be found online at <http://dx.doi.org/10.7717/peerj.8211#supplemental-information>.

REFERENCES

- Albert RM, Bamford MK, Cabanes D. 2006.** Taphonomy of phytoliths and macroplants in different soils from Olduvai Gorge (Tanzania) and the application to Plio-Pleistocene palaeoanthropological samples. *Quaternary International* **148**:78–94 DOI [10.1016/j.quaint.2005.11.026](https://doi.org/10.1016/j.quaint.2005.11.026).

- Albert RM, Bamford MK, Cabanes D. 2009.** Palaeoecological significance of palms at Olduvai Gorge, Tanzania, based on phytolith remains. *Quaternary International* **193**:41–48 DOI [10.1016/j.quaint.2007.06.008](https://doi.org/10.1016/j.quaint.2007.06.008).
- Albert RM, Bamford MK, Esteban I. 2015.** Reconstruction of ancient palm vegetation landscapes using a phytolith approach. *Quaternary International* **369**:51–66 DOI [10.1016/j.quaint.2014.06.067](https://doi.org/10.1016/j.quaint.2014.06.067).
- Albert RM, Marean C. 2012.** The exploitation of plant resources by early Homo sapiens: the phytolith record from Pinnacle Point 13B Cave, South Africa. *Geoarchaeology* **27**:363–384 DOI [10.1002/gea.21413](https://doi.org/10.1002/gea.21413).
- Albert RM, Ofer L, Estroff L, Weiner S, Tsatskin A, Ronen A, Lev-Yadun S. 1999.** Mode of occupation of Tabun Cave, Mt Carmel, Israel during the Mousterian period: a study of the sediments and phytoliths. *Journal of Archaeological Science* **26**:1249–1260 DOI [10.1006/jasc.1999.0355](https://doi.org/10.1006/jasc.1999.0355).
- Albert RM, Weiner S. 2001.** Study of opal phytoliths in prehistoric ash layers using a quantitative approach. In: Meunier J, Coline F, eds. *Phytoliths: applications in earth sciences and human history*. Lisse: Balkema, 251–266.
- Alexandre A, Meunier JD, Lézine AM, Vincens A, Schwartz D. 1997.** Phytoliths: indicators of grassland dynamics during the late Holocene in intertropical Africa. *Palaeogeography, Palaeoclimatology, Palaeoecology* **136**:213–229 DOI [10.1016/S0031-0182\(97\)00089-8](https://doi.org/10.1016/S0031-0182(97)00089-8).
- An X, Lu H, Chu G. 2015.** Surface soil phytoliths as vegetation and altitude indicators: a study from the southern Himalaya. *Scientific Reports* **5**:15523 DOI [10.1038/srep15523](https://doi.org/10.1038/srep15523).
- Anderson GD, Talbot LM. 1965.** Soil factors affecting the distribution of the grassland types and their utilization by wild animals on the Serengeti Plains, Tanganyika. *The Journal of Ecology* **53**:33–56.
- Arráiz H, Barboni D, Ashley G.M Mabulla, A, Baquedano E, Dominguez-Rodrigo M. 2017.** The FLK Zinj paleolandscape: reconstruction of a 1.84 Ma wooded habitat in the FLK Zinj-AMK-PTK-DS archaeological complex, Middle Bed I (Olduvai Gorge, Tanzania). *Palaeogeography, Palaeoclimatology, Palaeoecology* **488**:9–20 DOI [10.1016/j.palaeo.2017.04.025](https://doi.org/10.1016/j.palaeo.2017.04.025).
- Ashley GM, Barboni D, Dominguez-Rodrigo M, Bunn HT, Mabulla AZP, Diez-Martin F, Barba R, Baquedano E. 2010.** A spring and wooded habitat at FLK Zinj and their relevance to origins of human behavior. *Quaternary Research* **74**:304–314 DOI [10.1016/j.yqres.2010.07.015](https://doi.org/10.1016/j.yqres.2010.07.015).
- Bamford MK, Albert RM, Cabanes D. 2006.** Plio—Pleistocene macroplant fossil remains and phytoliths from Lowermost Bed II in the eastern palaeolake margin of Olduvai Gorge, Tanzania. *Quaternary International* **148**:95–112 DOI [10.1016/j.quaint.2005.11.027](https://doi.org/10.1016/j.quaint.2005.11.027).
- Barboni D. 2014.** Vegetation of Northern Tanzania during the Plio-Pleistocene: a synthesis of the paleobotanical evidences from Laetoli, Olduvai, and Peninj hominin sites. *Quaternary International* **322**:264–276.

- Barboni D, Ashley GM, Dominguez-Rodrigo M, Bunn HT, Mabulla AZ, Baquedano E. 2010.** Phytoliths infer locally dense and heterogeneous paleovegetation at FLK North and surrounding localities during upper Bed I time, Olduvai Gorge, Tanzania. *Quaternary Research* 74:344–354 DOI [10.1016/j.yqres.2010.09.005](https://doi.org/10.1016/j.yqres.2010.09.005).
- Barboni D, Bonnefille R, Alexandre A, Meunier JD. 1999.** Phytoliths as palaeoenvironmental indicators, West Side Middle Awash Valley, Ethiopia. *Palaeogeography, Palaeoclimatology, Palaeoecology* 152:87–100 DOI [10.1016/S0031-0182\(99\)00045-0](https://doi.org/10.1016/S0031-0182(99)00045-0).
- Barboni D, Bremond L. 2009.** Phytoliths of East African grasses: an assessment of their environmental and taxonomic significance based on floristic data. *Review of Palaeobotany and Palynology* 158:29–41 DOI [10.1016/j.revpalbo.2009.07.002](https://doi.org/10.1016/j.revpalbo.2009.07.002).
- Barboni D, Bremond L, Bonnefille R. 2007.** Comparative study of modern phytolith assemblages from inter-tropical Africa. *Palaeogeography, Palaeoclimatology, Palaeoecology* 246:454–470 DOI [10.1016/j.palaeo.2006.10.012](https://doi.org/10.1016/j.palaeo.2006.10.012).
- Beyene Y, Katoh S, WoldeGabriel G, Hart WK, Uto K, Sudo M, Kondo M, Hyodo M, Renne PR, Suwa G, Asfaw B. 2013.** The characteristics and chronology of the earliest Acheulean at Konso, Ethiopia. *Proceedings for the National Academy of Sciences of the United States of America* 110(5):1584–1591 DOI [10.1073/pnas.1221285110](https://doi.org/10.1073/pnas.1221285110).
- Bibi F, Kiessling W. 2015.** Continuous evolutionary change in Plio-Pleistocene mammals of eastern Africa. *Proceedings of the National Academy of Sciences of the United States of America* 112:10623–10628 DOI [10.1073/pnas.1504538112](https://doi.org/10.1073/pnas.1504538112).
- Bibi F, Pante M, Souron A, Stewart K, Varela S, Werdelin L, Boisserie JR, Fortelius M, Hlusko L, Njau J, De la Torre I. 2018.** Paleocology of the Serengeti during the Oldowan-Acheulean transition at Olduvai Gorge, Tanzania: the mammal and fish evidence. *Journal of Human Evolution* 120:48–75 DOI [10.1016/j.jhevol.2017.10.009](https://doi.org/10.1016/j.jhevol.2017.10.009).
- Blecker SW, McCulley RL, Chadwick OA, Kelly EF. 2006.** Biologic cycling of silica across a grassland bioclimate sequence. *Global Biogeochemical Cycles* 20:GB3023 DOI [10.1029/2006GB002690](https://doi.org/10.1029/2006GB002690).
- Blinnikov MS. 1994.** *Phytolith analysis and Holocene dynamics of alpine vegetation*. Vol. 115. Zürich: Veröffentlichungen des Geobotanischen Institutes der ETH, 23–40.
- Blinnikov MS. 2005.** Phytoliths in plants and soils of the interior Pacific Northwest, USA. *Review of Palaeobotany and Palynology* 135:71–98 DOI [10.1016/j.revpalbo.2005.02.006](https://doi.org/10.1016/j.revpalbo.2005.02.006).
- Blinnikov MS, Bagent CM, Reyerson PE. 2013.** Phytolith assemblages and opal concentrations from modern soils differentiate temperate grasslands of controlled composition on experimental plots at Cedar Creek, Minnesota. *Quaternary International* 287:101–113 DOI [10.1016/j.quaint.2011.12.023](https://doi.org/10.1016/j.quaint.2011.12.023).
- Blinnikov M, Busacca A, Whitlock C. 2002.** Reconstruction of the late Pleistocene grassland of the Columbia basin, Washington, USA, based on phytolith records in loess. *Palaeogeography, Palaeoclimatology, Palaeoecology* 177:77–101 DOI [10.1016/S0031-0182\(01\)00353-4](https://doi.org/10.1016/S0031-0182(01)00353-4).
- Blumenthal SA, Levin NE, Brown FH, Brugal JP, Chritz KL, Harris JM, Jehle GE, Cerling TE. 2017.** Aridity and hominin environments. *Proceedings of the*

- National Academy of Sciences of the United State of America* **114**:7331–7336
[DOI 10.1073/pnas.1700597114](https://doi.org/10.1073/pnas.1700597114).
- Bobe R, Behrensmeyer AK. 2004.** The expansion of grassland ecosystems in Africa in relation to mammalian evolution and the origin of the genus *Homo*. *Palaeogeography, Palaeoclimatology, Palaeoecology* **207**:399–420 [DOI 10.1016/j.palaeo.2003.09.033](https://doi.org/10.1016/j.palaeo.2003.09.033).
- Bonnefille B. 1995.** A reassessment of the Plio-Pleistocene pollen record of East Africa. In: Vrba E, Denton G, Partridge T, Burckle L, eds. *Paleoclimate and Evolution, with emphasis on human origins*. New Haven: Yale University Press, 299–310.
- Bonnefille R. 1984.** Palynological Research at Olduvai Gorge. *National Geographic Society Research Reports* **17**:227–242.
- Bozarth S. 1992.** Classification of opal phytoliths formed in selected dicotyledons native to the great plains. In: Rapp GJ, Mulholland SC, eds. *Phytolithic systematics: emerging issues*. New York: Plenum Press, 193–214.
- Bremond L, Alexandre A, Hély C, Guiot J. 2005.** A phytolith index as a proxy of tree cover density in tropical areas: calibration with Leaf Area Index along a forest–savanna transect in southeastern Cameroon. *Global and Planetary Change* **45**:277–293 [DOI 10.1016/j.gloplacha.2004.09.002](https://doi.org/10.1016/j.gloplacha.2004.09.002).
- Bremond L, Alexandre A, Wooller MJ, Hély C, Williamson D, Schäfer PA, Majule A, Guiot J. 2008.** Phytolith indices as proxies of grass subfamilies on East African tropical mountains. *Global and Planetary Change* **61**:209–224
[DOI 10.1016/j.gloplacha.2007.08.016](https://doi.org/10.1016/j.gloplacha.2007.08.016).
- Cahen L, Snehing NJ, Delhal J, Vail JR, Bonhomme M, Ledent D. 1984.** *The geochronology and evolution of Africa*. Oxford: Clarendon Press.
- Carnelli AL, Theurillat JP, Madella M. 2004.** Phytolith types and type-frequencies in subalpine–alpine plant species of the European Alps. *Review of Palaeobotany and Palynology* **129**:39–65 [DOI 10.1016/j.revpalbo.2003.11.002](https://doi.org/10.1016/j.revpalbo.2003.11.002).
- Cerling TE, Bowman JR, O’Neil JR. 1988.** An isotopic study of a fluvial-lacustrine sequence: the Plio-Pleistocene Koobi Fora sequence, East Africa. *Palaeogeography, Palaeoclimatology, Palaeoecology* **63**:335–356 [DOI 10.1016/0031-0182\(88\)90104-6](https://doi.org/10.1016/0031-0182(88)90104-6).
- Cerling TE, Wynn JG, Andanje SA, Bird MI, Korir DK, Levin NE, Macharia AN, Quade J, Remien CH. 2011.** Woody cover and hominin environments in the past 6 million years. *Nature* **476**:51–56 [DOI 10.1038/nature10306](https://doi.org/10.1038/nature10306).
- Clarke J. 2003.** The occurrence and significance of biogenic opal in the regolith. *Earth-Science Reviews* **60**:175–194 [DOI 10.1016/S0012-8252\(02\)00092-2](https://doi.org/10.1016/S0012-8252(02)00092-2).
- Collura LV, Neumann K. 2017.** Wood and bark phytoliths of West African woody plants. *Quaternary International* **43**:142–159.
- Copeland SR. 2007.** Vegetation and plant food reconstruction of lowermost Bed II, Olduvai Gorge, using modern analogues. *Journal of Human Evolution* **53**(2):146–175
[DOI 10.1016/j.jhevol.2007.03.002](https://doi.org/10.1016/j.jhevol.2007.03.002).
- Dawson JB. 1992.** Neogene tectonics and volcanicity in the North Tanzania sector of the Gregory Rift Valley: contrasts with the Kenya sector. *Tectonophysics* **204**:81–92
[DOI 10.1016/0040-1951\(92\)90271-7](https://doi.org/10.1016/0040-1951(92)90271-7).

- Deino AL. 2012.** 40Ar/39Ar dating of Bed I, Olduvai Gorge, Tanzania, and the chronology of early Pleistocene climate change. *Journal of Human Evolution* **63**:251–273 DOI [10.1016/j.jhevol.2012.05.004](https://doi.org/10.1016/j.jhevol.2012.05.004).
- EAMD East African Meteorological Department. 1967.** *The weather of East Africa*. Nairobi: National Government Publication.
- Eichhorn B, Neumann K, Garnier A. 2010.** Seed phytoliths in West African Comelinaceae and their potential for palaeoecological studies. *Palaeogeography, Palaeoclimatology, Palaeoecology* **298**(3–4):300–310.
- Esteban I, De Vynck JC, Singels E, Vlok J, Marean CW, Cowling RM, Fisher EC, Cabanes D, Albert RM. 2017.** Modern soil phytolith assemblages used as proxies for Paleoscape reconstruction on the south coast of South Africa. *Quaternary International* **434**:160–179 DOI [10.1016/j.quaint.2016.01.037](https://doi.org/10.1016/j.quaint.2016.01.037).
- Fahmy AG. 2008.** Diversity of lobate phytoliths in grass leaves from the Sahel region, West Tropical Africa: Tribe Paniceae. *Plant Systematics and Evolution* **270**:1–23 DOI [10.1007/s00606-007-0597-z](https://doi.org/10.1007/s00606-007-0597-z).
- Fick SE, Evett RR. 2018.** Distribution modelling of pre-Columbian California grasslands with soil phytoliths: new insights for prehistoric grassland ecology and restoration. *PLOS ONE* **13**:e0194315 DOI [10.1371/journal.pone.0194315](https://doi.org/10.1371/journal.pone.0194315).
- Fishkis O, Ingwersen J, Streck T. 2009.** Phytolith transport in sandy sediment: experiments and modeling. *Geoderma* **151**:168–178 DOI [10.1016/j.geoderma.2009.04.003](https://doi.org/10.1016/j.geoderma.2009.04.003).
- Foster A, Ebinger C, Mbede E, Rex D. 1997.** Tectonic development of the northern Taizaiian sector of the East African Rift System. *Journal of the Geological Society* **154**:689–700 DOI [10.1144/gsjgs.154.4.0689](https://doi.org/10.1144/gsjgs.154.4.0689).
- Fredlund GG, Egan D, Howell EA. 2001.** Inferring vegetation history from phytoliths. In: *The historical ecology handbook*. Washington, D.C.: Island Press.
- Fredlund GG, Tieszen LT. 1994.** Modern phytolith assemblages from the North American great plains. *Journal of Biogeography* **21**:321–335.
- Frost P. 1996.** The ecology of miombo woodlands. In: *The miombo in transition: woodlands and welfare in Africa*. 11–57.
- Gallego L, Distel RA. 2004.** Phytolith assemblages in grasses native to Central Argentina. *Annals of Botany* **94**:865–874 DOI [10.1093/aob/mch214](https://doi.org/10.1093/aob/mch214).
- Gao G, Jie D, Liu L, Liu H, Li D, Li N, Shi J, Leng C, Qiao Z. 2018a.** Assessment and calibration of representational bias in soil phytolith assemblages in Northeast China and its implications for paleovegetation reconstruction. *Quaternary Research* **90**:38–49 DOI [10.1017/qua.2018.5](https://doi.org/10.1017/qua.2018.5).
- Gao G, Jie D, Wang Y, Liu L, Liu H, Li D, Shi J, Leng C. 2018b.** Phytolith reference study for identifying vegetation changes in the forest—grassland region of northeast China. *Boreas* **47**:481–497 DOI [10.1111/bor.12280](https://doi.org/10.1111/bor.12280).
- Hay RL. 1976.** *Geology of Olduvai Gorge. A study of sedimentation in a semiarid basin*. Los Angeles: University of California Press.

- Herlocker DJ, Dirchl HJ. 1972.** Vegetation of Ngorongoro Conservation area, Tanzania. Canadian Wildlife Service Report Series no. 19. Ottawa: Canadian Wildlife Service Illustrations, maps Geog, 5, 39.
- Hodson MJ. 2016.** The development of phytoliths in plants and its influence on their chemistry and isotopic composition. Implications for palaeoecology and archaeology. *Journal of Archaeological Science* **68**:62–69 DOI [10.1016/j.jas.2015.09.002](https://doi.org/10.1016/j.jas.2015.09.002).
- Hodson MJ, White PJ, Mead A, Broadley MR. 2005.** Phylogenetic variation in the silicon composition of plants. *Annals of Botany* **96**:1027–1046 DOI [10.1093/aob/mci255](https://doi.org/10.1093/aob/mci255).
- Holmes A. 1951.** The sequence of Precambrian orogenic belts in south and central Africa. In: Sandiford KS, Blondel F, eds. *Proceedings of the 18th international geological congress*. London: Association of African Geological Surveys, 254–269.
- Honaine MF, Zucol AF, Osterrieth ML. 2009.** Phytolith analysis of Cyperaceae from the Pampean region, Argentina. *Australian Journal of Botany* **57**:512–523 DOI [10.1071/BT09041](https://doi.org/10.1071/BT09041).
- Hylland E, Smith SY, Sheldon ND. 2013.** Representational bias in phytoliths from modern soils of central North America: implications for paleovegetation reconstructions. *Palaeogeography Palaeoclimatology Palaeoecology* **374**:338–348 DOI [10.1016/j.palaeo.2013.01.026](https://doi.org/10.1016/j.palaeo.2013.01.026).
- Jager T. 1982.** *Soils of the Serengeti woodlands, Tanzania*. Wageningen: Pudoc.
- Kerns BK, Moore MM, Hart SC. 2001.** Estimating forest-grassland dynamics using soil phytolith assemblages and $\delta^{13}\text{C}$ of soil organic matter. *Ecoscience* **8**:478–488 DOI [10.1080/11956860.2001.11682678](https://doi.org/10.1080/11956860.2001.11682678).
- Kindt R, Breugel P, Van Lillesø JB, Bingham M, Demissew S, Dudley C, Friis I, Gachathi F, Kalema J, Mbago F, Minani V, Moshi H, Mulumba J, Namaganda M, Ndangalasi H, Ruffo C, Jamnadass R, Graudal LOV. 2011.** *Potential Natural Vegetation of Eastern Africa (Ethiopia, Kenya, Malawi, Rwanda, Tanzania, Uganda and Zambia) Forest & Landscape*. University of Copenhagen.
- Klopper RR, Chatelain C, Bänninger V, Steyn HM, De Wet BC, Arnold TH, Gautier L, Smith GF, Spichiger R. 2006.** Checklist of the flowering plants of Sub-Saharan Africa. An index of accepted names and synonyms. South African biodiversity network report. SABONET, Pretoria.
- Leakey MD. 1971.** Olduvai Gorge. In: *Excavations in Bed I and II, 1960–63*. Cambridge: Cambridge University Press.
- Leakey MD. 1979.** *Olduvai Gorge: my search for early man*. CIFOR, Bogor, Indonesia: HarperCollins.
- Leakey MD, Hay RL, Thurber DL, Protsch R, Berger R. 1972.** Stratigraphy, archaeology, and age of the Ndotu and Naisiusiu beds, Olduvai Gorge, Tanzania. *World Archaeology* **3**:328–341 DOI [10.1080/00438243.1972.9979514](https://doi.org/10.1080/00438243.1972.9979514).
- Leakey MD, Roe D. 1994.** *Olduvai Gorge: volume 5, excavations in beds III, IV and the Masek Beds (Vol. 5)*. Cambridge: Cambridge University Press.

- Lepre CJ, Roche H, Kent DV, Harmand S, Quinn RL, Brugal JP, Texier PJ, Enoble A, Feibel CS. 2011. An earlier origin for the Acheulean. *Nature* 477(7362):82–85 DOI 10.1038/nature10372.
- Levin NE, Brown FH, Behrensmeier AK, Bobe R, Cerling T. 2011. Paleosol carbonates from the Omo Group: isotopic records of local and regional environmental change in East Africa. *Palaeogeography, Palaeoclimatology, Palaeoecology* 307:75–89 DOI 10.1016/j.palaeo.2011.04.026.
- Levin NE, Quade J, Simpson S, Semaw S, Rogers M. 2004. Isotopic Evidence for Plio-Pleistocene Environmental Change at Gona, Ethiopia. *Earth and Planetary Science Letters* 219:93–110 DOI 10.1016/S0012-821X(03)00707-6.
- Lovett JC, Wasser SK. 1993. *Biogeography and ecology of the rain forests of eastern Africa*. Cambridge: Cambridge University Press.
- Lupien RL, Russell JM, Feibel C, Beck C, Castañeda I, Deino A, Cohen AS. 2018. A leaf wax biomarker record of early Pleistocene hydroclimate from West Turkana, Kenya. *Quaternary Science Reviews* 186:225–235 DOI 10.1016/j.quascirev.2018.03.012.
- Madella M, Alexandré A, Ball T. 2005. International code for phytolith nomenclature 1.0. *Annals of Botany* 96:253–260 DOI 10.1093/aob/mci172.
- Magill CR, Ashley GM, Freeman KH. 2013a. Ecosystem variability and early human habitats in eastern Africa. *Proceedings of the National Academy of Sciences of the United States of America* 110:1167–1174 DOI 10.1073/pnas.1206276110.
- Magill CR, Ashley GM, Freeman KH. 2013b. Water, plants, and early human habitats in eastern Africa. *Proceedings of the National Academy of Sciences of the United States of America* 110:1175–1180 DOI 10.1073/pnas.1209405109.
- Mercader J, Abtosway M, Baquedano E, Brid RW, Diez-Martin F, Dominquez-Rodrigo M, Favreau J, Itambu M, Lee P, Mabulla A, Patalano R. 2017. Starch contamination landscapes in field archaeology: Olduvai Gorge, Tanzania. *Boreas* 46(4):918–934 DOI 10.1111/bor.12241.
- Mercader J, Astudillo F, Barkworth M, Bennett T, Esselmont C, Kinyanjui R, Grossman DL, Simpson S, Walde D. 2010. Poaceae phytoliths from the Niassa Rift, Mozambique. *Journal of Archaeological Science* 37:1953–1967 DOI 10.1016/j.jas.2010.03.001.
- Mercader J, Bennett T, Esselmont C, Simpson S, Walde D. 2009. Phytoliths in woody plants from the Miombo woodlands of Mozambique. *Annals of Botany* 104:91–113 DOI 10.1093/aob/mcp097.
- Mercader J, Bennett T, Esselmont C, Simpson S, Walde D. 2011. Soil phytoliths from miombo woodlands in Mozambique. *Quaternary Research* 75:138–150 DOI 10.1016/j.yqres.2010.09.008.
- Mollet GF, Swisher III CC. 2012. The Ngorongoro Volcanic Highland and its relationships to volcanic deposits at Olduvai Gorge and East African Rift volcanism. *Journal of Human Evolution* 63:274–283 DOI 10.1016/j.jhevol.2011.09.001.
- Morris LR, Ryel RJ, West NE. 2010. Can soil phytolith analysis and charcoal be used as indicators of historic fire in the pinyon-juniper and sagebrush steppe

- ecosystem types of the Great Basin Desert, USA? *The Holocene* **20**:105–114
[DOI 10.1177/0959683609348858](https://doi.org/10.1177/0959683609348858).
- Murungi M.** 2017. Phytoliths at Sibudu (South Africa): implications for vegetation, climate, and human occupation during the MSA. PhD thesis, University of the Witwatersrand, Johannesburg.
- Neumann K, Fahmy AG, Müller-Scheeßel N, Schmidt M.** 2017. Taxonomic, ecological and palaeoecological significance of leaf phytoliths in West African grasses. *Quaternary International* **434**:15–32 [DOI 10.1016/j.quaint.2015.11.039](https://doi.org/10.1016/j.quaint.2015.11.039).
- Niboye EP.** 2010. Vegetation cover changes in ngorongoro conservation area from 1975 to 2000: the importance of remote sensing images. *The Open Geography Journal* **3**:15–27 [DOI 10.2174/1874923201003010015](https://doi.org/10.2174/1874923201003010015).
- Norton-Griffiths M, Herlocker D, Pennycuick L.** 1975. The patterns of rainfall in the Serengeti ecosystem, Tanzania. *African Journal of Ecology* **13**:347–374
[DOI 10.1111/j.1365-2028.1975.tb00144.x](https://doi.org/10.1111/j.1365-2028.1975.tb00144.x).
- Novello A, Bamford MK, Van Wijk Y, Wurz S.** 2018. Phytoliths in modern plants and soils from Klasies River, Cape Region (South Africa). *Quaternary International* **464**:440–459 [DOI 10.1016/j.quaint.2017.10.009](https://doi.org/10.1016/j.quaint.2017.10.009).
- Novello A, Barboni D, Berti-Equille L, Mazur JC, Poilecot P, Vignaud P.** 2012. Phytolith signal of aquatic plants and soils in Chad, Central Africa. *Review of Palaeobotany and Palynology* **178**:43–58 [DOI 10.1016/j.revpalbo.2012.03.010](https://doi.org/10.1016/j.revpalbo.2012.03.010).
- Peters CR, Blumenshine RJ.** 1995. Landscape perspectives on possible land use patterns for Early Pleistocene hominids in the Olduvai Basin, Tanzania. *Journal of Human Evolution* **29**(4):321–362 [DOI 10.1006/jhev.1995.1062](https://doi.org/10.1006/jhev.1995.1062).
- Piperno D.** 1988. *Phytolith analysis. An archaeological and geological perspective*. London: Academic Press.
- Piperno DR.** 2006. *Phytoliths: a comprehensive guide for archaeologists and paleoecologists*. Rowman Altamira.
- Piperno DR, Becker P.** 1996. Vegetational history of a site in the central Amazon basin derived from phytolith and charcoal records from natural soils. *Quaternary Research* **45**:202–209 [DOI 10.1006/qres.1996.0020](https://doi.org/10.1006/qres.1996.0020).
- Plummer TW, Ditchfield PW, Bishop LC, Kingston JD, Ferraro JV, Braun DR, Hertel F, Potts R.** 2009. Oldest evidence of toolmaking hominins in a grassland-dominated ecosystem. *PLOS ONE* **4**:e7199 [DOI 10.1371/journal.pone.0007199](https://doi.org/10.1371/journal.pone.0007199).
- Prassack KA, Pante MC, Njau JK, De la Torre I.** 2018. The paleoecology of Pleistocene birds from Middle Bed II, at Olduvai Gorge, Tanzania, and the environmental context of the Oldowan-Acheulean transition. *Journal of Human Evolution* **120**:32–47
[DOI 10.1016/j.jhevol.2017.11.003](https://doi.org/10.1016/j.jhevol.2017.11.003).
- Quinn RL, Lepre CJ, Wright JD, Feibel C.** 2007. Paleogeographic variations of pedogenic carbonate $\delta^{13}\text{C}$ values from Koobi Fora, Kenya: implications for floral compositions of Plio-Pleistocene hominin environments. *Journal of Human Evolution* **53**:560–573
[DOI 10.1016/j.jhevol.2007.01.013](https://doi.org/10.1016/j.jhevol.2007.01.013).

- Ravelo AC, Andreasen DH, Lyle M, Lyle AO, Wara MW. 2004.** Regional climate shifts caused by gradual global cooling in the Pliocene epoch. *Nature* **429(6989)**:263–267 DOI [10.1038/nature02567](https://doi.org/10.1038/nature02567).
- Rovner I. 1971.** Potential of opal phytoliths for use in paleoecological reconstruction. *Quaternary Research* **1**:343–359 DOI [10.1016/0033-5894\(71\)90070-6](https://doi.org/10.1016/0033-5894(71)90070-6).
- Runge F. 1999.** The opal phytolith inventory of soils in central Africa—quantities, shapes, classification, and spectra. *Review of Palaeobotany and Palynology* **107**:23–53 DOI [10.1016/S0034-6667\(99\)00018-4](https://doi.org/10.1016/S0034-6667(99)00018-4).
- Sinclair AR, Mduma SA, Hopcraft JG, Fryxell JM, Hilborn R, Thirgood S. 2007.** Long-term ecosystem dynamics in the Serengeti: lessons for conservation. *Conservation Biology* **21(3)**:580–590 DOI [10.1111/j.1523-1739.2007.00699.x](https://doi.org/10.1111/j.1523-1739.2007.00699.x).
- Sinclair ARE, Packer C, Mduma SA, Fryxell JM. 2008.** *Serengeti III: human impacts on ecosystem dynamics*. Chicago: University of Chicago Press.
- Sperazza M, Moore JN, Hendrix MS. 2004.** High-resolution particle size analysis of naturally occurring very fine-grained sediment through laser diffractometry. *Journal of Sedimentary Research* **74**:736–743 DOI [10.1306/031104740736](https://doi.org/10.1306/031104740736).
- Strömberg CA. 2004.** Using phytolith assemblages to reconstruct the origin and spread of grass-dominated habitats in the Great Plains of North America during the late Eocene to early Miocene. *Palaeogeography, Palaeoclimatology, Palaeoecology* **207**:239–275 DOI [10.1016/j.palaeo.2003.09.028](https://doi.org/10.1016/j.palaeo.2003.09.028).
- Strömberg CA, Di Stilio VS, Song Z. 2016.** Functions of phytoliths in vascular plants: an evolutionary perspective. *Functional Ecology* **30**:1286–1297 DOI [10.1111/1365-2435.12692](https://doi.org/10.1111/1365-2435.12692).
- Strömberg CA, Dunn RE, Crifo C, Harris EB. 2018.** Phytoliths in paleoecology: analytical considerations, current use, and future directions. In: Criff DA, Su DF, Simpson SW, eds. *Methods in Paleocology: reconstructing cenozoic terrestrial environments and ecological communities*. Switzerland: Springer, 235–287.
- Thorn VC. 2001.** Oligocene and Early Miocene phytoliths from CRP-2/2A and CRP-3, Victoria Land Basin, Antarctica. *Terra Antarctica* **8(4)**:407–422.
- Thorn VC. 2006.** Vegetation reconstruction from soil phytoliths, Tongariro National Park, New Zealand. *New Zealand Journal of Botany* **44**:397–413 DOI [10.1080/0028825X.2006.9513031](https://doi.org/10.1080/0028825X.2006.9513031).
- Tsartsidou G, Lev-Yadun S, Albert RM, Miller-Rosen A, Efstratiou N, Weiner S. 2007.** The phytolith archaeological record: strengths and weaknesses evaluated based on a quantitative modern reference collection from Greece. *Journal of Archaeological Science* **34**:1262–1275 DOI [10.1016/j.jas.2006.10.017](https://doi.org/10.1016/j.jas.2006.10.017).
- Twiss PC, Suess E, Smith RM. 1969.** Morphological classification of grass phytoliths 1. *Soil Science Society of America Journal* **33**:109–115 DOI [10.2136/sssaj1969.03615995003300010030x](https://doi.org/10.2136/sssaj1969.03615995003300010030x).
- Uno KT, Polissar PJ, Jackson KE. 2016.** Neogene biomarker record of vegetation change in eastern Africa. *Proceedings of the National Academy of Sciences of the United States of America* **113(23)**:6355–6363.

- Wallis L. 2003.** An overview of leaf phytolith production patterns in selected north-west Australian flora. *Review of Palaeobotany and Palynology* **125**:201–248
[DOI 10.1016/S0034-6667\(03\)00003-4](https://doi.org/10.1016/S0034-6667(03)00003-4).
- Watling J, Iriarte J, Whitney BS, Consuelo E, Mayle F, Castro W, Schaan D, Feldpausch TR. 2016.** Differentiation of neotropical ecosystems by modern soil phytolith assemblages and its implications for palaeoenvironmental and archaeological reconstructions II: Southwestern Amazonian forests. *Review of Palaeobotany and Palynology* **226**:30–43 [DOI 10.1016/j.revpalbo.2015.12.002](https://doi.org/10.1016/j.revpalbo.2015.12.002).
- White F. 1983.** *The vegetation of africa: a descriptive memoir to accompany the UNESCO/AETFAT/UNSO vegetation map of Africa*. Paris: Natural Resources Research. UNESCO.